Published in final edited form as:
Cell Metab. 2019 November 05; 30(5): 917–936.e10. doi:10.1016/j.cmet.2019.07.015.

Podoplanin-expressing macrophages promote lymphangiogenesis and lymphoinvasion via Galectin 8-mediated adhesion to tumor lymphatics

Paweł Bieniasz-Krzywiec[1,2,3,4], **Rosa Martín-Pérez**[1,2], **Manuel Ehling**[1,2], **Melissa García-Caballero**[5], **Sotiria Pinioti**[1,2], **Samantha Pretto**[1,2], **Roel Kroes**[1,2], **Chiara Aldeni**[1,2], **Mario Di Matteo**[1,2], **Hans Prenen**[2,6], **María Virginia Tribulatti**[7], **Oscar Campetella**[7], **Ann Smeets**[8], **Agnes Noel**[5], **Giuseppe Floris**[9], **Jo A. Van Ginderachter**[3,4], **Massimiliano Mazzone**[1,2,10,*]

[1]Laboratory of Tumor Inflammation and Angiogenesis, Center for Cancer Biology, VIB, Leuven, B3000, Belgium

[2]Laboratory of Tumor Inflammation and Angiogenesis, Center for Cancer Biology, Department of Oncology, KU Leuven, Leuven, B3000, Belgium.

[3]Myeloid Cell Immunology Lab, VIB Center for Inflammation Research, Brussels, B1050, Belgium

[4]Lab of Cellular and Molecular Immunology, Vrije Universiteit Brussel, Brussels B 1050, Belgium.

[5]Laboratory of Tumor and Developmental Biology, GIGA-Cancer, University of Liège, Sart-Tilman, B4000, Liège, Belgium.

[6]Oncology Department, University Hospital Antwerp, 2650, Edegem, Belgium.

[7]Institute for Research in Biotechnology, National University of San Martín, CONICET, Buenos Aires, 1650, Argentina

[8]Surgical Oncology Unit, Department of Oncology, KU Leuven, Leuven, B3000, Belgium.

[9]Translational Cell and Tissue Research Unit, Department of Imaging and Pathology, KU Leuven, Leuven, B3000, Belgium.

Summary

Among tumor-infiltrating immune cells, the highest expression of Podoplanin (PDPN) is found in a subset of tumor-associated macrophages (TAMs). We hereby demonstrate that PDPN is involved in the attachment of this TAM subset to lymphatic endothelial cells (LECs). Mechanistically, PDPN promotes β1 integrin activation in macrophages, mediating their binding to Galectin 8 (GAL8) expressed by LECs. When proximal to lymphatics, podoplanin-expressing macrophages (PoEMs) regulate local matrix remodeling and promote vessel growth and lymphoinvasion. Anti-integrin β1 blockade, macrophage-specific *Pdpn* knockout or GAL8 inhibition impair TAM adhesion to LECs. Such defective perilymphatic TAM recruitment restrains lymphangiogenesis and reduces lymphatic cancer spread. In breast cancer patients, association of PoEMs with tumor lymphatic vessels correlates with incidences of lymph node and distant organ metastasis.

[*]**Correspondence To**: massimiliano.mazzone@vib-kuleuven.be.
[10]Lead Contact

Europe PMC Funders Author Manuscripts

Keywords

podoplanin; tumor-associated macrophages; breast cancer; lymphangiogenesis; lymphoinvasion; lymph nodes; metastasis

Introduction

Despite numerous advances have been achieved in breast cancer treatment, the prognosis for patients with a metastatic disease remains poor, with a median survival of 2-4 years (Ayoub et al., 2012). Regional lymph nodes (LNs) are the primary sites of lymphatic drainage from all areas of the breast, and the extent of their involvement in breast cancer is a strong predictor of disease relapse and patient survival. Migration of cancer cells into the lymphatic circulation and entry into the LNs is greatly facilitated by tumor lymphangiogenesis, a process that generates new lymphatic vessels (LVs) from pre-existing conduits (Ran et al., 2010; Skobe et al., 2001). Clinical studies have shown that the production of lymphangiogenic factors and the occurrence of lymphangiogenesis correlate with disease outcome in various tumor types. Several soluble factors produced by lymphatic endothelial cells (LECs), cancer cells, or neighboring stromal cells have been implicated in the regulation of lymphangiogenesis and lymphoinvasion (including VEGFA, VEGFC, VEGFD, PDGFBB, and angiopoietins) (Stacker et al., 2014; Zheng et al., 2014).

Tumor-associated macrophages (TAMs) have critical roles at each stage of cancer progression (Mantovani, 2010; Nielsen and Schmid, 2017). However, the crosstalk between TAMs and lymphangiogenesis has not been extensively explored. One of the most relevant observation in the field is that TAM depletion in several tumor types abates VEGFC production and VEGFR3 signalling in LECs, thus impairing lymphangiogenesis (Ji et al., 2014). Nevertheless, molecular regulators of the interaction between TAMs and LECs are poorly characterized and specific TAM subsets facilitating cancer cell intravasation into the LVs remain unidentified.

PDPN (Podoplanin) is a small mucin-type transmembrane glycoprotein with a wide variety of functions, including regulation of cell motility and adhesion (Astarita et al., 2012). Physiologically, CLEC2/PDPN interaction facilitates blood and lymphatic vessel separation during embryogenesis (Uhrin et al., 2010). In adult mice, PDPN in LECs prevents retrograde blood filling into the lymphatic system but does not affect LV patterning and function in healthy organs. The upregulation of PDPN correlates with malignant progression in several tumors (Ugorski et al., 2016), including lymphatic metastasis in breast cancer (Braun et al., 2008). Despite being strongly expressed by LECs, PDPN is widely present in both cancer and tumor infiltrating cells, e.g. TAMs.

The roles of cancer cell-derived PDPN in tumor progression have been well documented (Cueni et al., 2010; Suzuki et al., 2010). Conversely, the function of PDPN-expressing macrophages (PoEMs) and the importance of this molecule in TAMs have never been explored. Given the fact that TAMs expressing certain blood endothelial cell (BEC) markers, such as TIE2 (De Palma and Naldini, 2011), VEGFR1 (Shibuya, 2006) and NRP1 (Casazza

Europe PMC Funders Author Manuscripts

et al., 2013) have already been implicated in angiogenesis, we wondered whether PDPN in macrophages plays a role in the growth of tumor lymphatics.

Results

Podoplanin-expressing macrophages (PoEMs) represent a perilymphatic TAM subset

Among all the cells of the immune system, we found that in orthotopic 4T1 breast tumors PDPN was almost exclusively expressed in TAMs but not in other tumor-infiltrating leukocytes, as assessed by FACS (Figure 1A). We also measured the transcript and protein levels of PDPN in different cell types, using freshly sorted tumor lymphatic endothelial cells (tLECs) as a reference. Strikingly, PDPN-expressing macrophages (PoEMs) had as much PDPN as tLECs (Figure 1B-1C). F4/80^{+} skin macrophages or circulating monocytes from these tumor-bearing mice were, respectively, scarcely positive or negative for PDPN (Figure S1A-S1B). In line, PoEMs were nearly absent in resected lymph nodes from both healthy and tumor-bearing mice (Figure S1C-S1D). These data suggest that PDPN expression becomes evident when monocytes differentiate into macrophages and experience some typical features of the tumor microenvironment such as hypoxia and/or TGFβ, which are known to promote *Pdpn* transcription (Suzuki et al., 2008; Tejchman et al., 2017).

Following, we characterized TAM heterogeneity and distribution within the tumoral space. PDPN^{+} TAMs (PoEMs) constituted about 30% of the entire TAM population infiltrating 4T1 breast tumors as shown by FACS (Figure 1D). Under histological assessment, we found that PoEMs were more proximal to the lymphatics than PDPN-negative TAMs (non-PoEMs) (Figure 1E-1G). Confocal imaging on thick sections from 4T1 breast tumors further confirmed that PoEMs localized in the proximity or adhered to the lymphatic vessel walls (Figure 1H). Next, we utilized the Rosa26.mTmG reporter line crossed with an inducible, macrophage specific *Csf1r*.iCre deleter, which allowed us to distinguish TAMs (EGFP^{+}) from all the other stromal components (Tomato^{+}). In the syngeneic E0771 orthotopic breast cancer model, we observed that round-shaped, PDPN^{+}, EGFP^{+} TAMs were found adjacent to the LV walls (Figure 1I).

When characterizing the PoEM phenotype, we observed that MHC II^{lo}/CD206^{hi} or CD11c^{-}/CD204^{hi} F4/80^{+} cells (pro-tumoral, M2-like) were highly positive for PDPN, while MHC II^{hi}/CD206^{lo} or CD11c^{+}/CD204^{lo} TAMs (anti-tumoral, M1-like) were PDPN-low or negative (Figure 1J-1K and Figure S1E-S1G) (Pucci et al., 2009). Besides, RNAseq analysis of PoEMs *vs.* PDPN-negative TAMs revealed more transcriptomic differences (accession number at the GEO database: GSE126722). Gene ontology (GO) enrichment analysis pointed at a highly significant upregulation (q value<0,005) of processes related to extracellular matrix (ECM) remodeling and reorganization in PoEMs. In contrast, GO terms related to growth factor and cytokine signalling did not show any significant changes (q value>0,005) (Figure S1H and not shown). Many matrix metalloproteinases (MMPs) and collagens, the main regulators of matrix organization and invasion (Barcus et al., 2017; Clark and Vignjevic, 2015) were found strongly upregulated in PoEMs *vs.* non-PoEMs (Figure 1L), while the majority of (lymph)angiogenic growth factors and cytokines did not show differential expression (Figure 1M). Overall, *Vegfc* and *Vegfd* (annotated as *Figf*), the two ligands of lymphangiogenic VEGFR3, were poorly expressed compared to

Vegfa (Figure S1I). These data suggest that PoEMs represent a subset of TAMs potentially involved in matrix turnover and invasion.

Pdpn deletion in TAMs inhibits tumor lymphatic growth and metastasis and impairs perilymphatic localization of TAMs

To study the biological function of PDPN in TAMs, WT and *Pdpn* KO bone marrow (BM) cells were used to reconstitute the immune system of lethally irradiated WT Balb/c recipient mice, thus generating WT→WT and *Pdpn* KO→WT chimerias (Figure S2A). Six weeks after BM reconstitution, syngeneic 4T1 breast cancer cells were injected orthotopically in both WT→WT and *Pdpn* KO→WT mice. Despite comparable tumor growth, pulmonary metastases were 60% lower in KO→WT *vs.* WT→WT mice (Figure 2A-2E and Figure S2B-S2C). This was not caused by differential cancer cell extravasation and lodging to the lungs, as the number of pulmonary nodules following intravenous injection of 4T1 cancer cells was comparable in WT→WT and KO→WT mice (Figure S2D). Similar to human triple-negative breast cancer (TNBC), 4T1 cancer cells disseminate preferentially via the lymphatic route, and to a lower extent via blood vessels (Mohammed et al., 2011; Pulaski and Ostrand-Rosenberg, 2001; Ran et al., 2010). We therefore focused our attention on tumor LVs and lymph node metastasis. Density, total area and lumen size of lymphatics were strongly (up to 75%) reduced in KO→WT *vs.* WT→WT mice, as assessed by the usage of various lymphatic endothelium markers *i.e.*, LYVE1, VEGFR3 and PROX1 (Figure 2F and Figure S2E-S2K). This impaired lymphangiogenesis was associated with decreased Evans Blue drainage from tumor to the inguinal lymph nodes (Figure S2L). Consistently, the number of $CK14^+$ breast cancer cells in the draining lymph nodes was 75% lower in KO→WT *vs.* WT→WT mice (Figure 2G-2H). On the other hand, tumor blood vessel density and area, as well as pericyte coverage, permeability and tumor hypoxia (parameters linked to cancer cell intravasation into the blood stream) (Mazzone et al., 2009) were not affected by *Pdpn* deletion (Figure S2M-S2S).

In order to further compare the rates of hematogenous and lymphatic dissemination, we assessed lung metastasis in WT→WT and KO→WT mice wherein the draining LNs were resected (or not) *prior* to orthotopic 4T1 tumor implantation. Lymph node resection in WT→WT mice reduced lung metastasis by 55% but it did not result in any additional effect in the KO→WT mice, suggesting that tumor blood vessel intravasation and hematogenous metastasis stayed unaltered (Figure 2I-2J). Consistent with our observation that PoEMs are absent in LNs, the blood or lymph vessel density in the draining lymph nodes of WT→WT and KO→WT tumor-bearing mice were the same (Figure S2T-S2V). Moreover, the injection of 4T1 cells directly into the draining LNs resulted in comparable lung metastasis (Figure S2W).

Based on the finding that PDPN in TAMs is relevant for LV growth and lymphatic metastasis, we hypothesized that standard anti-lymphangiogenic therapy would be ineffective in *Pdpn* KO→WT tumor-bearing mice. In WT→WT mice, a VEGFR3-blocking antibody (clone mF431C1) (Laakkonen et al., 2007) reduced 4T1 tumor lymph vessel formation and metastasis by 50% and 40%, respectively (Figure 2K-2N). However, anti-VEGFR3 had no effect on tumor lymphangiogenesis and dissemination in KO→WT

chimeras. Tumor growth was comparable in all the groups (Figure 2O). Altogether, these data indicate that PoEMs promote tumor lymphangiogenesis and lymphatic metastasis, likely favoring cancer cell entry into the lymphatic circulation.

As TAMs were the main population of leukocytes expressing PDPN (Figure 1A), we analyzed $CD11b^+$, $F4/80^+$ macrophages from 4T1 tumors (Figure S3A) and confirmed *Pdpn* deletion in KO→WT mice by both FACS and qRT-PCR (Figure S3B-S3C). *Pdpn* knockout did not influence overall TAM density (Figure S3D-S3E). However, the interaction of TAMs with LVs was strongly impaired in absence of PDPN (Figure 2P-2Q and Figure S3F). In contrast, TAM contact with tumor blood vessels did not change significantly in *Pdpn* WT *vs*. KO→WT mice (Figure S3G-S3H). Although PDPN was relevant for TAM attachment to the lymphatics, its deletion did not affect the expression of main M1 or M2 macrophage polarization markers, defining pro-inflammatory or pro-(lymph)angiogenic macrophage subsets, respectively (Figure S3I-S3L). Aligned, whole tumors and TAMs from *Pdpn* WT and KO chimeras had comparable expression of *Vegfa, Vegfc*, and *Vegfd* (Figure S3M-S3O). In line with the RNAseq data, while TAMs have high levels of *Vegfa*, they represent a smaller source of *Vegfc* and *Vegfd* as compared to the rest of the tumor.

In orthotopic EMT6.5 breast tumors, *Pdpn* KO TAMs also had impaired perilymphatic distribution, diminished LV area, and reduced metastatic burden, despite unaltered tumor growth (Figure S4A-S4H). Moreover, in mice lacking *Pdpn* specifically in TAMs upon Tamoxifen treatment (Figure 2R), orthotopic E0771 breast tumors displayed defective perilymphatic TAM localization (Figure 2S-2T and Figure S4I), as well as diminished lymphangiogenesis and metastasis, while tumor growth was comparable in all the groups (Figure 2U-2W and Figure S4J-S4O). Blood vessel density, pericyte coverage, tumor hypoxia and TAM infiltration were not altered by macrophage-specific *Pdpn* deletion (Figure S4P-S4U).

Finally, existing LVs in adult skin (Figure S5A-S6B), as well as pathological (lymph)angiogenesis in cauterized corneas (Figure S5C-S5F) were both comparable in WT→WT and KO→WT chimeras, consistent with the absence of PoEMs in these conditions (not shown). Overall, we found that PDPN expression is: *i)* the highest in pro-tumoral M2-like TAMs, *ii)* crucial for PoEM localization around the lymphatics, but *iii)* dispensable for determining their differentiation state into canonical M1 *vs*. M2 macrophages. By impairing the recruitment of a $PDPN^+$ TAM subset to the perilymphatic space, tumor lymphangiogenesis in KO→WT mice is reduced, with consequent drop of lymphatic metastasis.

Perilymphatic TAM localization is mediated by GAL8 expression in LECs

Given the perilymphatic localization defect of macrophages, we focused our attention on a known PDPN interactor − galectin 8 (GAL8), a secreted glycan-binding protein abundantly expressed by LVs, modulating cell adhesion and migration, codified by the gene *LGALS8* (Troncoso et al., 2014). First, we analyzed GAL8 expression in 4T1 tumor sections and found that this protein is expressed by tumor lymphatics and by some $CD45^+$ infiltrating immune cells, but not by tumor blood vessels (Figure 3A-3C). *In vitro*, LECs defined as $CD31^+$, $PDPN^+$ cells (Figure S6A) expressed *LGALS8* but did not express the most-studied

PDPN ligand − *CLEC2* (Figure S6B). In line with the *in vivo* distribution, *LGALS8* expression in cultured LECs was 3,2-times higher than in BECs (Figure S6C), and not detected in 4T1 or E0771 breast cancer cells (Figure S6D).

Next, we validated GAL8 binding to *Pdpn* WT bone marrow-derived macrophages (BMDMs), also expressing PDPN at the RNA and protein levels (Figure S6E-S6F). GAL8 binding was impaired by 70% in *Pdpn* KO BMDMs (Figure 3D-3E). When measuring the migratory capacity of macrophages in a Transwell assay, WT BMDMs migrated efficiently towards recombinant GAL8, whereas *Pdpn* KO BMDMs showed almost complete lack of migratory response (Figure 3F-3G). Interestingly, in the WT condition, the migrated BMDMs were PDPN-positive, whereas the non-migrated ones were negative for PDPN (Figure 3H-3I). This finding was consistent with the observation that macrophages differentiated *in vitro* from BM cells constitute a mixed population, in which about 20% of cells is PDPN-positive and the remaining 80% is PDPN-negative (Figure S6E). Furthermore, WT but not KO BMDMs were able to migrate towards a monolayer of LECs (Figures 3J). Silencing of *LGALS8* in LECs with three different siRNAs (or combinations of those) (Figure 3J-3L) or pharmacologic inhibition of GAL8 with thiodigalactoside (TDG) (Figure 3M) impaired the migration of WT BMDMs to the same extent as the knockout of *Pdpn*, but it did not further affect the migratory behavior of *Pdpn* KO macrophages. As a positive control, we show that the migratory capacity towards CCL2 was comparable for both WT and *Pdpn* KO BMDMs (Figure 3J). *LGALS8* reconstitution in silenced LECs restored macrophage chemoattraction, excluding possible off-target effects (Figure 3N and S6G-S6H). In line, *Pdpn* deficiency strongly impaired the *ex vivo* migration of sorted TAMs towards GAL8 (Figure 3O-3P). Therefore, our data demonstrate that GAL8 expression by the LVs is important for macrophage migration to LECs.

In order to validate the significance of lymphatic vessel-derived GAL8 for TAM recruitment into the perilymphatic space, we generated a pseudo-specific knockout of GAL8 in tumor lymphatics. To this end, *Lgals8* WT and KO recipient mice were reconstituted with BM cells from *Csf1r*.iCre x *Pdpn*$^{lox/lox}$ mice (or from *Csf1r*.iCre x *Pdpn*$^{wt/wt}$ controls) (Figure 4A). Since in tumors GAL8 was expressed by leukocytes and lymphatics only (Figure 3A-3C), this procedure restricted *Lgals8* deficiency to LVs, whereas CD45^{+} immune cells still expressed GAL8 (Figure 4B). Genetic deletion of *Lgals8* in LECs strongly decreased tumor lymphatic vessel area and the attachment of *Pdpn* WT TAMs to tumor lymphatics (Figure 4C-4E). This was accompanied by a reduction in lung metastasis (Figure 4F-4G). Conversely, *Lgals8* deletion in the context of *Pdpn* KO TAMs did not further affect tumor LVs, perilymphatic TAM distribution or the metastatic burden observed in *Pdpn* KO chimeras. All experimental groups showed comparable tumor growth (Figure 4H).

Next, we utilized TDG in order to provide a proof-of-concept of pharmacologic GAL8 targeting, even though TDG is not a specific GAL8 inhibitor as its mode of action also restrains Galectin 1, Galectin 3, and Galectin 9 (Tribulatti et al., 2012). In this approach, we chose another breast cancer model - 4T1 (instead of E0771 tumors as in the abovementioned genetic targeting). Intratumoral injection of TDG (Ito et al., 2011) in WT→WT mice led to similar effects as those observed in the *Lgals8* KO recipients, namely to decreased lymphangiogenesis, less TAM-LV interactions and reduced lung metastasis (Figure 4I-4N).

In *Pdpn* KO→WT mice, TDG treatment did not additionally influence the lymphatic phenotype. Although galectins can affect blood vessel formation and $CD8^+$ T cell activation (Ito et al., 2011; Markowska et al., 2010), tumor growth, tumor blood vessel density, or $CD8^+$ T cell infiltration were not influenced by TDG treatment in our model (Figures 4O-4S). Altogether, these data argue that GAL8 in breast tumor lymphatics and PDPN in TAMs participate in the same molecular process and emerge as key factors of a previously unexplored metastatic cascade in breast cancer.

PoEM migration and adhesion depend on GAL8-mediated integrin β1 activation

GAL8 binding to PDPN was reported to favor clustering and activation of integrin β1 (CD29) in LECs (Chen et al., 2016). Given the adhesion defects observed in *Pdpn* KO BMDMs, we wondered whether similar effects occur on PoEM (macrophage) surfacewe. Indeed, we found that GAL8 stimulation induced integrin β1 activation in *Pdpn* WT but not in KO BMDMs (Figure 5A-5B) and that GAL8 binding to *Itgb1*-silenced BMDMs was decreased to the same level as in *Pdpn* KO BMDMs (Figure S6I-S6K). No additional impairment of GAL8 binding was observed upon silencing of integrin β1 in *Pdpn* KO BMDMs. Next, we found that PDPN and β1 integrin interaction was promoted by GAL8 stimulation in *Pdpn* WT but not in *Pdpn* KO BMDMs, as assessed by a proximity ligation assay (PLA) (Figure 5C-5D) and co-immunoprecipitation for PDPN and integrin β1 subunit (Figure S6L). In line with the fact that integrin β1 signaling is crucial for macrophage migration (Meng and Lowell, 1998), the deactivation of β1 on WT BMDMs (with a blocking antibody or with siRNAs) impaired their *in vitro* adhesion to LECs (Figure 5E-5F) or their migration towards GAL8 (Figure 5G). This effect was specifically dependent on integrin β1, but not on integrin β2 (Figure S6M-S6O). Altogether, these data support the idea that the binding of GAL8 to PDPN on macrophage surface promotes the formation of a multicomplex with β1 integrin and ultimately its activation − a prerequisite for macrophage migration and adhesion to LECs.

PDPN-mediated adhesion of PoEMs to LECs promotes lymphatic growth and cancer cell lymphoinvasion

To assess the functional relevance of our findings, we conducted a capillary network formation assay where *Pdpn* WT or KO BMDMs were seeded together with LECs. In these conditions, LECs cultured with *Pdpn* KO BMDMs formed simpler, less dense lymphatic networks in comparison to those observed in the presence of WT BMDMs (Figure S6P-S6Q). Then, using a 3D sprouting assay in a type I collagen gel, we demonstrated that BMDMs increase the number and length of sprouts observed in spheroids of LECs alone. Moreover, this lymphangiogenic effect was much stronger when the same assay was performed by adding PoEMs to the spheroid (instead of a total BMDM pool) (Figure 5H-5J). Neither *Pdpn* KO nor PDPN-negative BMDMs elicited any sprouting effect. In contrast, PoEMs, non-PoEMs, total *Pdpn* WT and KO BMDMs triggered a similar proliferative boost when co-cultured with LECs (Figure S6R); LEC apoptosis was scarce and not increased in any of the conditions tested (Figure S6S). Altogether, these data indicate that PDPN in PoEMs is important for sustaining lymphatic vessel sprouting but not for LEC proliferation and survival.

Macrophage proximity to blood vessels has been shown to modulate endothelial junctions and favor blood vessel intravasation of cancer cells through their direct interaction, resulting in the formation of TAM-cancer cell-BEC triads (Harney et al., 2015). We therefore set up a system where we evaluated how different sorted populations of F4/80$^+$ BMDMs were remodeling VE-cadherin junctions of a confluent LEC monolayer. We found that the opening of the endothelial layer was much stronger in the presence of PDPN$^+$ macrophages but not with PDPN$^-$ or *Pdpn* KO macrophages (Figure 5K-5L). Aligned with these results, transendothelial migration of Calcein-labelled 4T1 cancer cells was promoted by PDPN$^+$ but not by PDPN$^-$ or *Pdpn* KO macrophages (Figure 5M). Pre-incubation of macrophages with the integrin β1 blocker prevented PoEM-induced formation of interendothelial gaps and 4T1 cancer cell transmigration (Figure 5K-5M). Thus, PoEM adhesion to the lymphatic endothelium is sufficient to induce gaps in a LEC monolayer and facilitate cancer cell transmigration.

In light of the above findings, we assessed the presence of triads at the lymphatic vessel site by implanting GFP-expressing 4T1 tumors into BM chimeras. In WT→WT mice, clusters of LECs, macrophages and a GFP+ cancer cells were frequently found, while their presence was reduced by 35 % in the KO→WT mice (even when normalized for strongly reduced LV area) (Figure 5N-5O and Figure S6T-S6U). Together, these data suggest that PoEMs at the LVs are instrumental for the promotion of lymphatic growth and cancer cell lymphoinvasion.

PDPN in PoEMs serves as an upstream regulator of matrix remodeling

Based on the initial RNAseq-based observations (Figure 1L and Figure S1H), we hypothesized that PDPN could be involved upstream in the transcriptional regulation of certain genes. We arbitrarily focused on the top 100 upregulated (and not downregulated) transcripts (FDR<0,05), taking into account the mediators of matrix composition and digestion i.e., collagens and MMPs, located at the right side of the volcano plot (Figure 1L). We identified a list of 4 MMPs (*Mmp2, Mmp9, Mmp12, Mmp13*) and 8 collagen subunit genes (*Col1a1, Col1a2, Col3a1, Col5a2, Col5a3, Col5a1, Col6a2, Col6a3*) which were highly upregulated in PoEMs *vs*. non-PoEMs. Using independent cohorts of mice, we confirmed that PoEMs had the highest expression levels of all these genes, while non-PoEMs, *Pdpn* WT and KO TAMs showed lower transcript values (Figure 6A-6M). *Vegfa, Vegfc*, and *Vegfd* were equally expressed in both PoEMs and non-PoEMs as well as in their total pool, and their expression did not change in *Pdpn* KO TAMs (Figure 6N-6P).

Lymphatic capillaries attach directly to interstitial matrix, mainly composed of fibrillar type I collagen (Detry et al., 2011). Interestingly, PoEMs, constituting a TAM subset proximal to tumor lymphatics, abundantly express *Col1a1* and *Col1a2* subunits. Consistently, bundles of type I collagen were richly deposited by *ex vivo* cultured PoEMs, and less by PDPN-negative TAMs and *Pdpn* KO TAMs, while total *Pdpn* WT TAMs displayed an intermediate collagen I deposition state, as assessed by stainings on the decellularized matrix (Figure 6Q-6R). Histologically, 4T1 tumor sections had thinner sleeves of type I collagen around LVs in KO→WT *vs*. WT→WT mice (Figure 6S-6T).

CTX-I are C-terminal telopeptides that are released during type I collagen digestion (Garnero et al., 2003). Consistent with the highest levels of *Mmp2, Mmp9, Mmp12,*

Mmp13 (and other MMPs that were further down in the list of upregulated genes), PoEMs displayed the strongest collagen degradation activity (Figure 6U) and the highest gelatinase activity, the latter ascribed to MMP2, MMP9 and MMP12 (Chelluboina et al., 2015; Jacob et al., 2013; Li et al., 2012) (Figure 6V). Consistently, tumor LVs in the KO→WT mice had 60% less perilymphatic MMP12 accumulation than in WT→WT mice (Figure 6W-6X). In tumors, matrix remodeling and MMPs offer new paths for migration and invasion, but also allow the release of growth factors that otherwise would remain bound to matrix components, to the cell surface, or sequestered by growth-factor binding proteins (Bergers et al., 2000; Mott and Werb, 2004). In line, our next observations revealed that soluble *vs*. matrix-bound VEGFC and VEGFD ratios (main lymphangiogenic growth factors) were much lower in *ex vivo* cultured *Pdpn* KO TAMs than in WT TAMs (despite comparable protein levels in WT and KO TAM extracts, or in whole tumors from WT→WT and KO→WT mice) (Figure 6Y-6Z and Figure S7A-S7D). This suggests that the chemoattractant capacity of these growth factors (and possibly of many others) is reduced in KO→WT mice, as impaired matrix remodeling makes them poorly available in solution. Of note, TAMs constitute a very poor source of VEGFC as compared to other cellular components in 4T1 tumors (Figure S7E).

To assess if the transcriptional regulation of MMPs and type I collagens depended on GAL8, we analyzed PoEMs, PDPN-negative TAMs and total TAMs isolated from *Lgals8* total KO mice, thus preventing any interaction between PDPN and GAL8 *in vivo*. Under these conditions we could still appreciate the upregulation of *Mmp9, Mmp12, Mmp13, Col1a1* and *Col1a2* in PoEMs *vs*. non-PoEMs, whereas the absence of GAL8 did not influence this expression pattern (Figure S7F-S7K). Lymphangiogenic genes i.e., *Vegfa, Vegfc a*nd *Vegfd*, were instead comparable in all sorted populations, suggesting that neither PDPN nor GAL8 was impacting on their transcription levels (Figure S7L-S7N). Overall, PDPN in TAMs appear to be not only instrumental for favoring the proximity of PoEMs to tumor LVs, but it also regulates the extracellular matrix (ECM) turnover by enhancing collagen formation and degradation. Hence, PoEMs promote lymphangiogenesis and lymphoinvasion both directly by remodeling the matrix in the proximity of growing tumor LVs, and indirectly by favoring growth factor liberation and accessibility.

Potential clinical relevance of PoEMs in breast cancer patients

Finally, we translated these findings to human breast cancer patients. Like in murine tumors, 30% of the TAMs expressed PDPN (as assessed in a small cohort of patients) (Figure 8A). Furthermore, freshly sorted human PoEMs, but not PDPN-negative TAMs, carried the ability to migrate towards soluble GAL8 (Figure 8B). Likewise,, human monocyte-derived $PDPN^+$ macrophages had enhanced ability to migrate towards LECs, as compared to non-PoEMs (Figures 8C). This migratory capability was lost when LECs were silenced for *LGALS8*. Finally, we analyzed tumor samples from a unique cohort of patients with bilateral synchronous breast tumors, in which one tumor was lymph node positive (N+), while the contralateral tumor was lymph node negative (N0). Adhesion of $PDPN^+$ TAMs to the lymphatic walls correlated with the presence of metastasized regional tumor LNs (p value range = 0,00037– 0,049). In patients with bilateral tumors that were both N0, we could not observe differences in the number of $PDPN^+$ TAMs interacting with the lymphatic vessel

walls (Figure 8D-8F). When analyzing the N+ subgroup, patients with both LN and organ metastasis (N+,M+) had significantly higher numbers of PoEMs per tumor lymphatic vessel than patients with lymph node metastasis but no organ metastasis (N+, M0) (Figure 8G). All together, we demonstrate that PoEMs are present in human breast cancer and that, due to their response to LEC-derived GAL8, they localize in direct proximity to tumor lymphatics. Our data represent a proof-of-concept of PoEMs as a potential prognostic marker in breast cancer patients.

Discussion

The general understanding on how macrophages influence lymphangiogenesis pinpoints to their production and release of growth factors and metalloproteases (Mantovani, 2010; Noel et al., 2008). However, the mechanisms whereby TAMs interact and participate in the formation of lymphatic conduits within the tumor, as well as their impact on cancer cell lymphoinvasion, are not well understood. One of the recently identified mechanisms describes integrin β4 as the molecule retaining a minor fraction of macrophages proximal to lymphatic endothelium in *ex vivo* assays. Those macrophages stimulate LEC contraction and remodeling via the release of TGF-β1, which could have implications for lymphatic metastasis (Evans et al., 2019). On the other hand, we demonstrate here (by reporting mouse and human data) that PDPN in TAMs engages β1 integrin during the recruitment and adhesion of these cells to GAL8 expressed by lymphatics. Once in the perilymphatic space, Podoplanin-expressing macrophages promote ECM remodeling (independently of GAL8 binding), enhancing lymphangiogenesis and metastasis in both direct (by stimulating lymphatic growth and cancer cell intravasation) and indirect way (through the liberation of VEGFC and VEGFD from the matrix). Specifically, PDPN defines the localization of TAMs around the lymphatic sprouts, but it is also instrumental for matrix remodeling through the transcriptional regulation of MMPs and collagens. As GAL8 induces macrophage migration towards lymphatics but does not impact on the expression of ECM-related genes, this transcriptional regulation depends on PDPN but not on GAL8. Hence, we speculate that PDPN expression *per se* is sufficient to induce the translocation of certain transcriptional factors into the nucleus. For example, human pleural mesothelioma cells with high levels of PDPN display active, nuclear YAP1; conversely, PDPN inhibition prevents YAP1 activation (Takeuchi et al., 2017). In line, YAP1 has been already described as a transcriptional regulator of collagen (especially type I collagen) and MMPs (Kegelman et al., 2018; Nukuda et al., 2015). Alternatively, a PDPN interactor different from GAL8 might be responsible for the regulation of these transcriptional cascades. *Vice versa*, we cannot exclude that GAL8 is enhancing MMP activity post-transcriptionally and independently of PDPN, for example through its physical interaction with pro-MMP9 (Nishi et al., 2003), or indirectly, through transactivation of EGFR signalling in other cells *e.g.*, cancer cells (Oyanadel et al., 2018).

Upon stimulation with GAL8, PDPN in LECs activates VEGFC/VEGFR3-dependent and independent signals through the clustering of α1β1/ α5β1 integrins (Chen et al., 2016). By using two models of corneal lymphangiogenesis i.e., allogenic corneal transplantation and HSV infection, this previous study has indicated that global *Lgals8* KO and *Pdpn* KO mice display defective lymphatic sprouting in response to VEGFC. As indicated by *in vitro* assays and *in vivo* cornea stainings, in some physiopathological conditions GAL8 is exclusively

expressed by inflammatory cells and binds to PDPN on the LVs. Our study reveals further that, in tumors, PDPN induction in TAMs overtakes the function of PDPN in LECs as simultaneous inhibition of GAL8 and macrophage-derived *Pdpn* does not additionally impede tumor lymphangiogenesis.

In lymphangiogenesis, ECM remodeling is of high importance as, in contrast to BECs (that lean on a basement membrane), LECs are in direct contact with the interstitial matrix and lack (or have incomplete) basement membrane. Hence, matrix formation and degradation, as well as matrix stiffness, mechanically modulate the ability of cancer cells to migrate and invade LVs. Furthermore, ECM remodeling, or MMPs in general, increase the release of several growth factors (such as VEGF, HGF, FGF, IGF and others), promoting their chemoattractant potential on neighboring cells *e.g.*, cancer cells and LECs (Mott and Werb, 2004; Bergers et al., 2000). Here, we show that proximity and adhesion of PoEMs to the lymphatics correlates with matrix remodeling and reorganization enforced by a local production of MMPs and collagens. Despite the fact that other stromal cells could have higher proteolytic activity than $PDPN^+$ TAMs (as for example tumor-associated neutrophils) or produce a higher extent of collagens (as cancer-associated fibroblasts), GAL8/integrin β1-mediated adhesion of PoEMs to the LV wall creates a topographic distribution of matrix remodeling enzymes and enriches the perilymphatic niche with active lymphangiogenic and growth factors. It follows that relocating TAMs out of the perilymphatic space by knocking out *Pdpn* will likely not affect the overall levels of proteases, matrix bundles and growth factors in the tumor, but it will rather result in a lower concentration of all these proteins around LVs. In contrast, we show that PoEMs are adjacent to lymphatic vessels but do not integrate into the vessel wall, at least in murine models of breast cancer. Overall, these data support the idea that changes in specific tumor niches can affect cancer progression and therapeutic outcomes (Casazza et al., 2013; Stockmann et al., 2008).

Because of the high up-regulation of various collagen subunits and MMPs by PoEMs v*ersus* non-PoEMs, the properties of ECM around tumor LVs differ between WT and *Pdpn* KO chimeras. It has been well-recognized that the deregulation of ECM is a hallmark of cancer and a factor promoting dissemination (Jena and Janjanam, 2018). Specifically, during breast cancer development, collagen I stiffens the ECM, which promotes tumor invasion and metastasis (Conklin et al., 2011; Zhu et al., 2014). Furthermore, collagen I accelerates lymphatic regeneration and wound repair, supporting its role in the control of lymphatic function (Clavin et al., 2008). Collagen I fiber density was also found increased in lymph node-positive breast cancers (Kakkad et al., 2012). In line, various members of the MMP family were identified as poor prognosis markers for breast cancer patients (Radisky and Radisky, 2015). MMPs directly facilitate cancer dissemination by degrading the basement membrane. They can also directly impact on cancer cells, releasing growth factors and suppressing apoptosis (Gialeli et al., 2011). Importantly, MMP-mediated blood and lymph vessel formation and generation of tissue disruptive fibrotic stroma provides routes for the spreading of breast cancer (Kessenbrock et al., 2010). Finally, MMPs can directly induce epithelial-mesenchymal transition in breast cancer cells (Nistico et al., 2012; Radisky and Radisky, 2010).

Europe PMC Funders Author Manuscripts

In two different mouse models of breast cancer, a subset of TAMs, namely TEMs ($TIE2^+$ TAMs), has been shown to favor hematogenous metastasis by promoting vascular hyper-permeability and cancer cell dissemination in both pre-malignant lesions and late carcinomas (Harney et al., 2015; Linde et al., 2018). Analogically, here we identify and characterize a subset of TAMs, namely PoEMs, that is relevant for lymphoinvasion - the main dissemination route in human TNBC (Mohammed et al., 2011). Our study shows that the presence of PDPN on a specific TAM subset is important for: *i)* selective macrophage attachment to the lymphatic wall and not blood vessel wall, *ii)* LV growth and lymphatic dissemination (via formation of triads of LECs, TAMs and cancer cells), likely due to *iii)* increased matrix remodeling *per se* and, indirectly, by *iv)* enhancing growth factor liberation and accessibility. The remodeled ECM, as well as a bunch of various growth factors that are virtually liberated by PoEMs, do not necessarily origin from PoEMs themselves but can be initially produced by other stromal cells, immune cells or cancer cells.

PoEMs are barely found in normal skin or in wounded corneas. This is in line with a study in breast cancer patients, showing that TEMs in tumors but not in adjacent normal tissues express specific lymphatic markers including PDPN (Bron et al., 2016). Similar to what has been shown for TIE2 in TEMs, we demonstrate here that PDPN (originally a lymphatic lineage marker) is responsible for the adhesion of a TAM fraction to the tumor lymphatic endothelium. In spite of the similarities between TEMs and PoEMs, our RNAseq analysis of end-stage 4T1 breast tumors indicates that PoEMs do not express *Tie2/Tek* and are therefore distinct from TEMs.

Unlike VEGFC that plays an essential role in lymphatic homeostasis as well as in physiological and pathological angiogenesis, the pathway we describe in this study may hold specificity for tumor lymphangiogenesis, therefore circumventing possible side effects (such as lymphoedema) observed in patients and mice treated with anti-VEGFC or anti-VEGFR3 antibodies. Moreover, PDPN-targeted therapies embrace the opportunity to block multiple other cell types and biological processes in cancer, such as the interaction of cancer-associated fibroblasts with cancer cells (Shindo et al., 2013), dendritic cell trafficking (Acton et al., 2012), collective migration of cancer cells (Shen et al., 2010), and regulatory T cell development and T cell exhaustion (Fuertbauer et al., 2013). We also validate that genetic or pharmacologic blockade of GAL8 prevents PoEM proximity to the LVs, thus reducing tumor lymphangiogenesis and metastatic dissemination. These observations pave the venue towards the screening and the use of PDPN and GAL8-specific inhibitors or blocking antibodies in cancer therapy. Even more clinically relevant, the analysis of PoEMs in a tumor could be an indication for complete lymph node resection or for adjuvant chemotherapy. Larger cohorts of patients are warranted to further explore this idea. From a broader perspective, our findings underpin the possibility to generate *in vitro* PoEMs to enable lymphangiogenesis and lymphatic drainage in case of lymphedema, as it often occurs upon breast cancer treatment, in obesity or in congenital diseases *e.g.*, in Milroy disease.

Supplementary Material

Refer to Web version on PubMed Central for supplementary material.

References

Acton SE, Astarita JL, Malhotra D, Lukacs-Kornek V, Franz B, Hess PR, Jakus Z, Kuligowski M, Fletcher AL, Elpek KG, et al. Podoplanin-rich stromal networks induce dendritic cell motility via activation of the C-type lectin receptor CLEC-2. Immunity. 2012; 37: 276–289. DOI: 10.1016/j.immuni.2012.05.022 [PubMed: 22884313]

Astarita JL, Acton SE, Turley SJ. Podoplanin: emerging functions in development, the immune system, and cancer. Front Immunol. 2012; 3: 283. doi: 10.3389/fimmu.2012.00283 [PubMed: 22988448]

Ayoub JP, Verma S, Verma S. Advances in the management of metastatic breast cancer: options beyond first-line chemotherapy. Curr Oncol. 2012; 19: 91–105. DOI: 10.3747/co.19.1024 [PubMed: 22514495]

Barcus CE, O'Leary KA, Brockman JL, Rugowski DE, Liu Y, Garcia N, Yu M, Keely PJ, Eliceiri KW, Schuler LA. Elevated collagen-I augments tumor progressive signals, intravasation and metastasis of prolactin-induced estrogen receptor alpha positive mammary tumor cells. Breast Cancer Res. 2017; 19: 9. doi: 10.1186/s13058-017-0801-1 [PubMed: 28103936]

Bergers G, Brekken R, McMahon G, Vu TH, Itoh T, Tamaki K, Tanzawa K, Thorpe P, Itohara S, Werb Z, et al. Matrix metalloproteinase-9 triggers the angiogenic switch during carcinogenesis. Nat Cell Biol. 2000; 2: 737–744. DOI: 10.1038/35036374 [PubMed: 11025665]

Braun M, Flucke U, Debald M, Walgenbach-Bruenagel G, Walgenbach KJ, Holler T, Polcher M, Wolfgarten M, Sauerwald A, Keyver-Paik M, et al. Detection of lymphovascular invasion in early breast cancer by D2-40 (podoplanin): a clinically useful predictor for axillary lymph node metastases. Breast Cancer Res Treat. 2008; 112: 503–511. [PubMed: 18165897]

Bron S, Henry L, Faes-Van't Hull E, Turrini R, Vanhecke D, Guex N, Ifticene-Treboux A, Marina Iancu E, Semilietof A, Rufer N, et al. TIE-2-expressing monocytes are lymphangiogenic and associate specifically with lymphatics of human breast cancer. Oncoimmunology. 2016; 5 e1073882 doi: 10.1080/2162402X.2015.1073882 [PubMed: 27057438]

Casazza A, Laoui D, Wenes M, Rizzolio S, Bassani N, Mambretti M, Deschoemaeker S, Van Ginderachter JA, Tamagnone L, Mazzone M. Impeding macrophage entry into hypoxic tumor areas by Sema3A/Nrp1 signaling blockade inhibits angiogenesis and restores antitumor immunity. Cancer Cell. 2013; 24: 695–709. [PubMed: 24332039]

Chelluboina B, Warhekar A, Dillard M, Klopfenstein JD, Pinson DM, Wang DZ, Veeravalli KK. Post-transcriptional inactivation of matrix metalloproteinase-12 after focal cerebral ischemia attenuates brain damage. Sci Rep. 2015; 5 9504 doi: 10.1038/srep09504 [PubMed: 25955565]

Chen WS, Cao Z, Sugaya S, Lopez MJ, Sendra VG, Laver N, Leffler H, Nilsson UJ, Fu J, Song J, et al. Pathological lymphangiogenesis is modulated by galectin-8-dependent crosstalk between podoplanin and integrin-associated VEGFR-3. Nat Commun. 2016; 7 11302 doi: 10.1038/ncomms11302 [PubMed: 27066737]

Clark AG, Vignjevic DM. Modes of cancer cell invasion and the role of the microenvironment. Curr Opin Cell Biol. 2015; 36: 13–22. [PubMed: 26183445]

Clavin NW, Avraham T, Fernandez J, Daluvoy SV, Soares MA, Chaudhry A, Mehrara BJ. TGF-beta1 is a negative regulator of lymphatic regeneration during wound repair. Am J Physiol Heart Circ Physiol. 2008; 295: H2113–2127. [PubMed: 18849330]

Conklin MW, Eickhoff JC, Riching KM, Pehlke CA, Eliceiri KW, Provenzano PP, Friedl A, Keely PJ. Aligned collagen is a prognostic signature for survival in human breast carcinoma. Am J Pathol. 2011; 178: 1221–1232. DOI: 10.1016/j.ajpath.2010.11.076 [PubMed: 21356373]

Cueni LN, Hegyi I, Shin JW, Albinger-Hegyi A, Gruber S, Kunstfeld R, Moch H, Detmar M. Tumor lymphangiogenesis and metastasis to lymph nodes induced by cancer cell expression of podoplanin. Am J Pathol. 2010; 177: 1004–1016. DOI: 10.2353/ajpath.2010.090703 [PubMed: 20616339]

De Palma M, Naldini L. Angiopoietin-2 TIEs up macrophages in tumor angiogenesis. Clin Cancer Res. 2011; 17: 5226–5232. [PubMed: 21576085]

Detry B, Bruyere F, Erpicum C, Paupert J, Lamaye F, Maillard C, Lenoir B, Foidart JM, Thiry M, Noel A. Digging deeper into lymphatic vessel formation in vitro and in vivo. BMC Cell Biol. 2011; 12: 29. doi: 10.1186/1471-2121-12-29 [PubMed: 21702933]

Evans R, Flores-Borja F, Nassiri S, Miranda E, Lawler K, Grigoriadis A, Monypenny J, Gillet C, Owen J, Gordon P, et al. Integrin-Mediated Macrophage Adhesion Promotes Lymphovascular Dissemination in Breast Cancer. Cell Rep. 2019; 27: 1967–1978. e1964 doi: 10.1016/j.celrep.2019.04.076 [PubMed: 31091437]

Fuertbauer E, Zaujec J, Uhrin P, Raab I, Weber M, Schachner H, Bauer M, Schutz GJ, Binder BR, Sixt M, et al. Thymic medullar conduits-associated podoplanin promotes natural regulatory T cells. Immunol Lett. 2013; 154: 31–41. [PubMed: 23912054]

Garnero P, Ferreras M, Karsdal MA, Nicamhlaoibh R, Risteli J, Borel O, Qvist P, Delmas PD, Foged NT, Delaisse JM. The type I collagen fragments ICTP and CTX reveal distinct enzymatic pathways of bone collagen degradation. J Bone Miner Res. 2003; 18: 859–867. [PubMed: 12733725]

Gialeli C, Theocharis AD, Karamanos NK. Roles of matrix metalloproteinases in cancer progression and their pharmacological targeting. FEBS J. 2011; 278: 16–27. [PubMed: 21087457]

Harney AS, Arwert EN, Entenberg D, Wang Y, Guo P, Qian BZ, Oktay MH, Pollard JW, Jones JG, Condeelis JS. Real-Time Imaging Reveals Local, Transient Vascular Permeability, and Tumor Cell Intravasation Stimulated by TIE2hi Macrophage-Derived VEGFA. Cancer Discov. 2015; 5: 932–943. DOI: 10.1158/2159-8290.CD-15-0012 [PubMed: 26269515]

Ito K, Scott SA, Cutler S, Dong LF, Neuzil J, Blanchard H, Ralph SJ. Thiodigalactoside inhibits murine cancers by concurrently blocking effects of galectin-1 on immune dysregulation, angiogenesis and protection against oxidative stress. Angiogenesis. 2011; 14: 293–307. DOI: 10.1007/s10456-011-9213-5 [PubMed: 21523436]

Jacob A, Jing J, Lee J, Schedin P, Gilbert SM, Peden AA, Junutula JR, Prekeris R. Rab40b regulates trafficking of MMP2 and MMP9 during invadopodia formation and invasion of breast cancer cells. J Cell Sci. 2013; 126: 4647–4658. DOI: 10.1242/jcs.126573 [PubMed: 23902685]

Jena MK, Janjanam J. Role of extracellular matrix in breast cancer development: a brief update. F1000Res. 2018; 7: 274. doi: 10.12688/f1000research.14133.2 [PubMed: 29983921]

Ji H, Cao R, Yang Y, Zhang Y, Iwamoto H, Lim S, Nakamura M, Andersson P, Wang J, Sun Y, et al. TNFR1 mediates TNF-alpha-induced tumour lymphangiogenesis and metastasis by modulating VEGF-C-VEGFR3 signalling. Nat Commun. 2014; 5 4944 [PubMed: 25229256]

Kakkad SM, Solaiyappan M, Argani P, Sukumar S, Jacobs LK, Leibfritz D, Bhujwalla ZM, Glunde K. Collagen I fiber density increases in lymph node positive breast cancers: pilot study. J Biomed Opt. 2012; 17 116017 doi: 10.1117/1.JBO.17.11.116017 [PubMed: 23117811]

Kegelman CD, Mason DE, Dawahare JH, Horan DJ, Vigil GD, Howard SS, Robling AG, Bellido TM, Boerckel JD. Skeletal cell YAP and TAZ combinatorially promote bone development. FASEB J. 2018; 32: 2706–2721. DOI: 10.1096/fj.201700872R [PubMed: 29401582]

Kessenbrock K, Plaks V, Werb Z. Matrix metalloproteinases: regulators of the tumor microenvironment. Cell. 2010; 141: 52–67. DOI: 10.1016/j.cell.2010.03.015 [PubMed: 20371345]

Laakkonen P, Waltari M, Holopainen T, Takahashi T, Pytowski B, Steiner P, Hicklin D, Persaud K, Tonra JR, Witte L, et al. Vascular endothelial growth factor receptor 3 is involved in tumor angiogenesis and growth. Cancer Res. 2007; 67: 593–599. [PubMed: 17234768]

Li J, Wang JJ, Peng Q, Chen C, Humphrey MB, Heinecke J, Zhang SX. Macrophage metalloelastase (MMP-12) deficiency mitigates retinal inflammation and pathological angiogenesis in ischemic retinopathy. PLoS One. 2012; 7 e52699 doi: 10.1371/journal.pone.0052699 [PubMed: 23285156]

Linde N, Casanova-Acebes M, Sosa MS, Mortha A, Rahman A, Farias E, Harper K, Tardio E, Reyes Torres I, Jones J, et al. Macrophages orchestrate breast cancer early dissemination and metastasis. Nat Commun. 2018; 9 21 doi: 10.1038/s41467-017-02481-5 [PubMed: 29295986]

Mantovani A. Molecular pathways linking inflammation and cancer. Curr Mol Med. 2010; 10: 369–373. [PubMed: 20455855]

Markowska AI, Liu FT, Panjwani N. Galectin-3 is an important mediator of VEGF-and bFGF-mediated angiogenic response. J Exp Med. 2010; 207: 1981–1993. DOI: 10.1084/jem.20090121 [PubMed: 20713592]

Mazzone M, Dettori D, de Oliveira RL, Loges S, Schmidt T, Jonckx B, Tian YM, Lanahan AA, Pollard P, de Almodovar CR, et al. Heterozygous deficiency of PHD2 restores tumor oxygenation

and inhibits metastasis via endothelial normalization. Cell. 2009; 136: 839–851. DOI: 10.1016/j.cell.2009.01.020 [PubMed: 19217150]

Meng F, Lowell CA. A beta 1 integrin signaling pathway involving Src-family kinases, Cbl and PI-3 kinase is required for macrophage spreading and migration. EMBO J. 1998; 17: 4391–4403. DOI: 10.1093/emboj/17.15.4391 [PubMed: 9687507]

Mohammed RA, Ellis IO, Mahmmod AM, Hawkes EC, Green AR, Rakha EA, Martin SG. Lymphatic and blood vessels in basal and triple-negative breast cancers: characteristics and prognostic significance. Mod Pathol. 2011; 24: 774–785. [PubMed: 21378756]

Mott JD, Werb Z. Regulation of matrix biology by matrix metalloproteinases. Curr Opin Cell Biol. 2004; 16: 558–564. DOI: 10.1016/j.ceb.2004.07.010 [PubMed: 15363807]

Nielsen SR, Schmid MC. Macrophages as Key Drivers of Cancer Progression and Metastasis. Mediators Inflamm. 2017; 2017 9624760 doi: 10.1155/2017/9624760 [PubMed: 28210073]

Nishi N, Shoji H, Seki M, Itoh A, Miyanaka H, Yuube K, Hirashima M, Nakamura T. Galectin-8 modulates neutrophil function via interaction with integrin alphaM. Glycobiology. 2003; 13: 755–763. [PubMed: 12881409]

Nistico P, Bissell MJ, Radisky DC. Epithelial-mesenchymal transition: general principles and pathological relevance with special emphasis on the role of matrix metalloproteinases. Cold Spring Harb Perspect Biol. 2012; 4 doi: 10.1101/cshperspect.a011908 [PubMed: 22300978]

Noel A, Jost M, Maquoi E. Matrix metalloproteinases at cancer tumor-host interface. Semin Cell Dev Biol. 2008; 19: 52–60. [PubMed: 17625931]

Nukuda A, Sasaki C, Ishihara S, Mizutani T, Nakamura K, Ayabe T, Kawabata K, Haga H. Stiff substrates increase YAP-signaling-mediated matrix metalloproteinase-7 expression. Oncogenesis. 2015; 4 e165 doi: 10.1038/oncsis.2015.24 [PubMed: 26344692]

Oyanadel C, Holmes C, Pardo E, Retamal C, Shaughnessy R, Smith P, Cortes P, Bravo-Zehnder M, Metz C, Feuerhake T, et al. Galectin-8 induces partial epithelial-mesenchymal transition with invasive tumorigenic capabilities involving a FAK/EGFR/proteasome pathway in Madin-Darby canine kidney cells. Mol Biol Cell. 2018; 29: 557–574. DOI: 10.1091/mbc.E16-05-0301 [PubMed: 29298841]

Pucci F, Venneri MA, Biziato D, Nonis A, Moi D, Sica A, Di Serio C, Naldini L, De Palma M. A distinguishing gene signature shared by tumor-infiltrating Tie2-expressing monocytes, blood “resident” monocytes, and embryonic macrophages suggests common functions and developmental relationships. Blood. 2009; 114: 901–914. [PubMed: 19383967]

Pulaski BA, Ostrand-Rosenberg S. Mouse 4T1 breast tumor model. Curr Protoc Immunol. 2001; 20 (20) 22. [PubMed: 18432775]

Radisky ES, Radisky DC. Matrix metalloproteinase-induced epithelial-mesenchymal transition in breast cancer. J Mammary Gland Biol Neoplasia. 2010; 15: 201–212. DOI: 10.1007/s10911-010-9177-x [PubMed: 20440544]

Radisky ES, Radisky DC. Matrix metalloproteinases as breast cancer drivers and therapeutic targets. Front Biosci (Landmark Ed). 2015; 20: 1144–1163. DOI: 10.2741/4364 [PubMed: 25961550]

Ran S, Volk L, Hall K, Flister MJ. Lymphangiogenesis and lymphatic metastasis in breast cancer. Pathophysiology. 2010; 17: 229–251. DOI: 10.1016/j.pathophys.2009.11.003 [PubMed: 20036110]

Shen Y, Chen CS, Ichikawa H, Goldberg GS. SRC induces podoplanin expression to promote cell migration. J Biol Chem. 2010; 285: 9649–9656. DOI: 10.1074/jbc.M109.047696 [PubMed: 20123990]

Shibuya M. Vascular endothelial growth factor receptor-1 (VEGFR-1/Flt-1): a dual regulator for angiogenesis. Angiogenesis. 2006; 9: 225–230. [PubMed: 17109193]

Shindo K, Aishima S, Ohuchida K, Fujiwara K, Fujino M, Mizuuchi Y, Hattori M, Mizumoto K, Tanaka M, Oda Y. Podoplanin expression in cancer-associated fibroblasts enhances tumor progression of invasive ductal carcinoma of the pancreas. Mol Cancer. 2013; 12: 168. doi: 10.1186/1476-4598-12-168 [PubMed: 24354864]

Skobe M, Hawighorst T, Jackson DG, Prevo R, Janes L, Velasco P, Riccardi L, Alitalo K, Claffey K, Detmar M. Induction of tumor lymphangiogenesis by VEGF-C promotes breast cancer metastasis. Nat Med. 2001; 7: 192–198. [PubMed: 11175850]

Stacker SA, Williams SP, Karnezis T, Shayan R, Fox SB, Achen MG. Lymphangiogenesis and lymphatic vessel remodelling in cancer. Nat Rev Cancer. 2014; 14: 159–172. [PubMed: 24561443]

Stockmann C, Doedens A, Weidemann A, Zhang N, Takeda N, Greenberg JI, Cheresh DA, Johnson RS. Deletion of vascular endothelial growth factor in myeloid cells accelerates tumorigenesis. Nature. 2008; 456: 814–818. DOI: 10.1038/nature07445 [PubMed: 18997773]

Suzuki H, Kato Y, Kaneko MK, Okita Y, Narimatsu H, Kato M. Induction of podoplanin by transforming growth factor-beta in human fibrosarcoma. FEBS Lett. 2008; 582: 341–345. [PubMed: 18158922]

Suzuki H, Onimaru M, Yonemitsu Y, Maehara Y, Nakamura S, Sueishi K. Podoplanin in cancer cells is experimentally able to attenuate prolymphangiogenic and lymphogenous metastatic potentials of lung squamoid cancer cells. Mol Cancer. 2010; 9: 287. doi: 10.1186/1476-4598-9-287 [PubMed: 21034514]

Takeuchi S, Fukuda K, Yamada T, Arai S, Takagi S, Ishii G, Ochiai A, Iwakiri S, Itoi K, Uehara H, et al. Podoplanin promotes progression of malignant pleural mesothelioma by regulating motility and focus formation. Cancer Sci. 2017; 108: 696–703. DOI: 10.1111/cas.13190 [PubMed: 28182302]

Tejchman A, Lamerant-Fayel N, Jacquinet JC, Bielawska-Pohl A, Mleczko-Sanecka K, Grillon C, Chouaib S, Ugorski M, Kieda C. Tumor hypoxia modulates podoplanin/CCL21 interactions in CCR7+ NK cell recruitment and CCR7+ tumor cell mobilization. Oncotarget. 2017; 8: 31876–31887. DOI: 10.18632/oncotarget.16311 [PubMed: 28416768]

Tribulatti MV, Figini MG, Carabelli J, Cattaneo V, Campetella O. Redundant and antagonistic functions of galectin-1, -3, and -8 in the elicitation of T cell responses. J Immunol. 2012; 188: 2991–2999. [PubMed: 22357632]

Troncoso MF, Ferragut F, Bacigalupo ML, Cardenas Delgado VM, Nugnes LG, Gentilini L, Laderach D, Wolfenstein-Todel C, Compagno D, Rabinovich GA, et al. Galectin-8: a matricellular lectin with key roles in angiogenesis. Glycobiology. 2014; 24: 907–914. [PubMed: 24939370]

Ugorski M, Dziegiel P, Suchanski J. Podoplanin - a small glycoprotein with many faces. Am J Cancer Res. 2016; 6: 370–386. [PubMed: 27186410]

Uhrin P, Zaujec J, Breuss JM, Olcaydu D, Chrenek P, Stockinger H, Fuertbauer E, Moser M, Haiko P, Fassler R, et al. Novel function for blood platelets and podoplanin in developmental separation of blood and lymphatic circulation. Blood. 2010; 115: 3997–4005. [PubMed: 20110424]

Zheng W, Aspelund A, Alitalo K. Lymphangiogenic factors, mechanisms, and applications. J Clin Invest. 2014; 124: 878–887. DOI: 10.1172/JCI71603 [PubMed: 24590272]

Zhu J, Xiong G, Trinkle C, Xu R. Integrated extracellular matrix signaling in mammary gland development and breast cancer progression. Histol Histopathol. 2014; 29: 1083–1092. DOI: 10.14670/hh-29.1083 [PubMed: 24682974]

Europe PMC Funders Author Manuscripts

Europe PMC Funders Author Manuscripts

Significance

We demonstrate that macrophage-derived PDPN retains PoEMs in close association with lymphatic vessels through its interaction with GAL8 on the lymphatic endothelium. Once there, PoEMs stimulate lymphangiogenesis and form triads with cancer cells and LECs, facilitating lymphatic dissemination to local lymph nodes by their increased capacity to promote matrix remodeling. The impact of our findings lies in the following aspects: *i)* we characterize a TAM subset supporting specifically tumor lymphangiogenesis and lymphoinvasion, *ii)* we show that perilymphatic release of matrix components, matrix-remodeling enzymes and, indirectly, of growth factors is important for these processes. Consequently, PDPN, PoEMs, and GAL8 might constitute potential prognostic biomarkers and could open up new therapeutic opportunities for the inhibition of lymphatic metastasis in breast cancer patients.

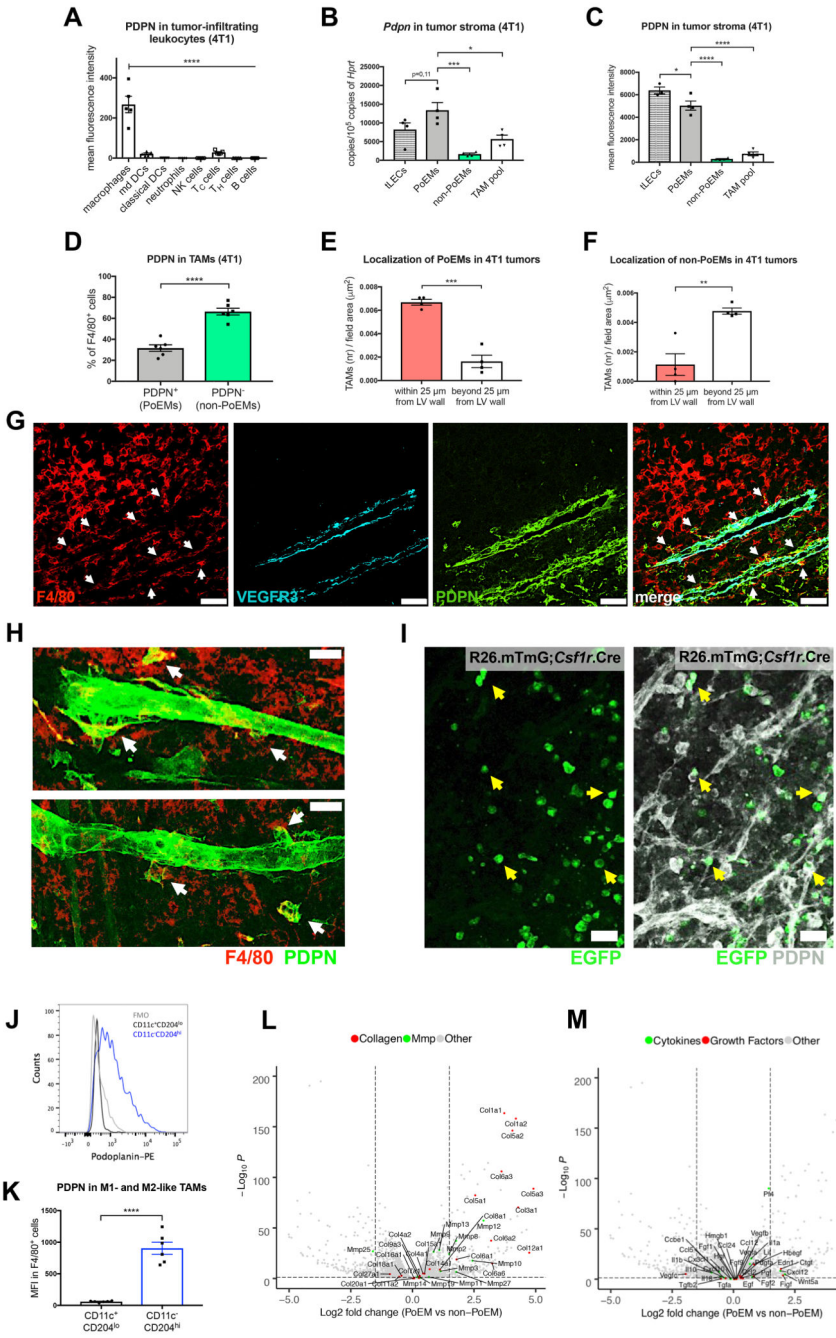

Figure 1. Podoplanin-expressing macrophages (PoEMs) represent a perilymphatic TAM subset.

(A-D) FACS analysis of the expression of PDPN in 4T1 tumor-infiltrating CD45$^+$ immune cells: macrophages (CD11b$^+$, F4/80$^+$), monocyte-derived DCs (CD11b$^+$, CD11c$^+$, F4/80$^-$), classical DCs (CD11b$^-$, CD11c$^+$), neutrophils (CD11b$^+$, Ly6G$^+$), NK cells (NKp46$^+$), cytotoxic T cells (TCRβ$^+$, CD4$^-$, CD8$^+$), T helper cells (TCRβ$^+$, CD4$^+$, CD8$^-$) and B cells (CD19$^+$) **(A)**. qRT-PCR analysis of the expression of *Pdpn* mRNA in stromal populations sorted from 4T1 tumors: LECs (CD45$^-$, CD31$^+$, PDPN$^+$), PoEMs (CD45$^+$, CD11b$^+$, F4/80$^+$, PDPN$^+$), non-PoEMs (CD45$^+$, CD11b$^+$, F4/80$^+$, PDPN$^-$) and total TAM pool (CD45$^+$,

CD11b^{+}, F4/80^{+}) **(B)**. FACS analysis of the expression of PDPN in stromal populations in 4T1 tumors: LECs (CD45^{-}, CD31^{+}, PDPN^{+}), PoEMs (CD45^{+}, CD11b^{+}, F4/80^{+}, PDPN^{+}), non-PoEMs (CD45^{+}, CD11b^{+}, F4/80^{+}, PDPN^{-}) and total TAM pool (CD45^{+}, CD11b^{+}, F4/80^{+}) **(C)**. FACS analysis of PDPN^{+} (PoEMs) and PDPN^{-} (non-PoEMs) fractions in 4T1 TAMs (CD11b^{+}, F4/80^{+}) **(D)**.

(**E-F**) Immunofluorescent analysis of the localization of F4/80^{+}, PDPN^{+} **(E)** or F4/80^{+}, PDPN^{-} **(F)** TAMs next to PDPN^{+}, VEGFR3^{+} LVs (within a distance of 25 μm from lymphatic vessel wall) and far from PDPN^{+}, VEGFR3^{+} LVs in 4T1 tumors. The number of cells was normalized per counting area (μm^{2}).

(G) Representative images of the localization of F4/80^{+}, PDPN^{+} (white arrows) or F4/80^{+}, PDPN^{-} TAMs in the proximity and far from PDPN^{+}, VEGFR3^{+} LVs in 4T1 tumors bore by WT→WT chimeras.

(H) Representative confocal images of 100 μm 4T1 tumor sections demonstrating F4/80^{+}, PDPN^{+} TAMs (white arrows) in close proximity to PDPN^{+} LVs.

(I) Representative confocal images of thick E0771 tumor sections implanted in ROSA$^{mT/mG}$;*Csf1r*:iCre mice, demonstrating EGFP^{+}, PDPN^{+} macrophages (yellow arrows) in the proximity but not incorporated into PDPN^{+} LVs. mT/mG, membrane-Tomato/membrane-GFP.

(J-K) FACS analysis of the expression of PDPN in 4T1-derived TAM (CD11b^{+}, F480^{+}) populations, namely M1-like (CD11c^{hi}, CD204^{lo}) and M2-like (CD11c^{lo}, CD204^{hi}). Similar results were obtained when gating for MHC II and CD206 for M1-like and M2-like populations (see Figure S1E-S1G).

(L-M) Volcano plots showing the transcript distribution for several collagen subunits and MMPs **(L)** or cytokines and growth factors **(M)**. The logarithms of the fold changes of individual genes (x axis) are plotted against the negative logarithm of their p-value to base 10 (y axis). Positive log2 (fold change) values represent upregulation in PoEMs (sorted as triple positive cells for CD11b, F4/80, PDPN) compared to non-PoEMs (CD11b^{+}, F4/80^{+}, PDPN^{-} cells) out of the same tumor sample. Negative values represent downregulation. Dots above the horizontal dashed line represent differentially expressed genes with p<0,05 after correction for multiple testing.

Statistical analysis: *P<0,05; **P<0,005; ***P<0,0005; ****P<0,00005. Graphs show mean ± standard error of the mean (SEM). Scale bars: 50 μm **(G, H, I)**. DC, dendritic cells; PoEMs, Podoplanin-expressing macrophages; non-PoEMs, Podoplanin-negative macrophages; TAMs, tumor-associated macrophages; tLECs, tumor lymphatic endothelial cells.

Europe PMC Funders Author Manuscripts

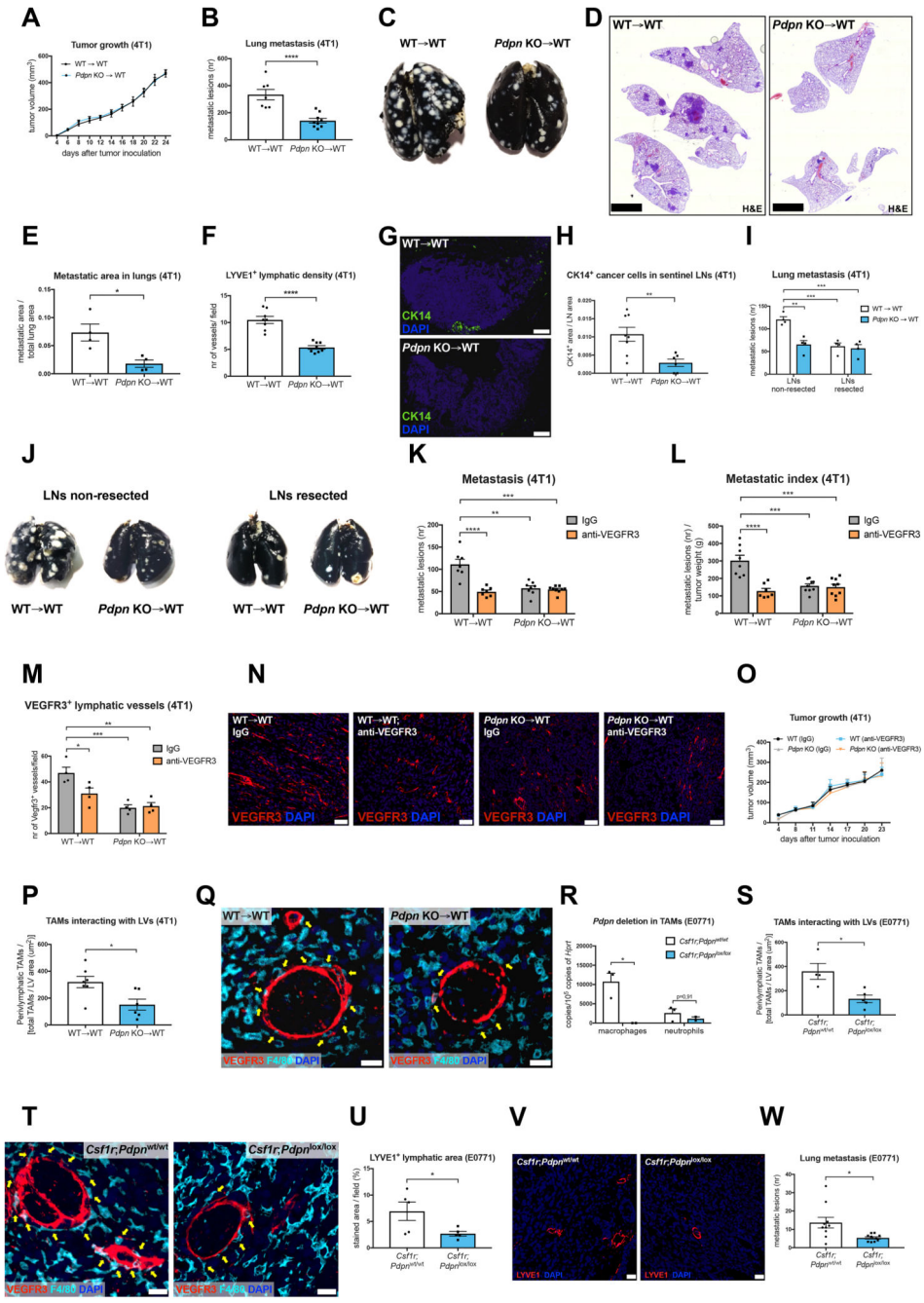

Figure 2. Deletion of PDPN in TAMs inhibits tumor lymphatic growth and metastasis.

(A-E) 4T1 tumor growth **(A)**, lung metastasis **(B)**, representative images of black ink-injected lungs from 4T1 tumor-bearing mice **(C)**, representative images of lung sections stained with hematoxylin-eosin (H&E) **(D)** and histologically assessed metastatic area in lungs **(E)** of WT→WT or *Pdpn* KO→WT chimeras. Data show representative values of 4 independent experiments.

(F) Quantifications of 4T1 tumor sections stained for a lymphatic endothelial cell specific marker LYVE1.

Europe PMC Funders Author Manuscripts

(G-H) Representative images and quantifications of inguinal lymph nodes from 4T1 tumor-bearing mice, stained for cytokeratin 14 (CK14) as a marker of cancer cells.
(I-J) Quantification of lung metastasis **(I)** and representative images of black ink-injected lungs **(J)** from mice in which lymphadenectomy of tumor-draining lymph nodes was performed 7 days prior to 4T1 cell inoculation.
(K-O) Quantification of lung metastasis **(K)**, metastatic index **(L)**, $VEGFR3^+$ lymphatics in tumors **(M)**, representative images of tumor sections stained for VEGFR3 **(N)** and 4T1 tumor growth **(O)** in WT→WT and *Pdpn* KO→WT mice treated with a VEGFR3-blocking antibody (Mf431C1) or with an isotype (rat IgG) control by bi-weekly intratumoral injections (40 μg per 1 g of body weight).
(P-Q) Quantification **(P)** and representative images **(Q)** of $F4/80^+$ TAMs (yellow arrows) directly interacting with $VEGFR3^+$ LVs in 4T1 tumors.
(R) qRT-PCR for *Pdpn* mRNA in $CD11b^+$, $F4/80^+$ TAMs and $CD11b^+$, $Ly6G^+$ neutrophils isolated from E0771 tumors bore by $Csf1r;Pdpn^{wt/wt}$ or $Csf1r;Pdpn^{lox/lox}$ mice.
(S-T) Quantification **(S)** and representative images **(T)** of $F4/80^+$ TAMs (yellow arrows) directly interacting with $VEGFR3^+$ LVs in E0771 tumors.
(U-V) Quantification **(U)** and representative images **(V)** of E0771 tumor sections stained for a lymphatic endothelial cell specific marker LYVE1.
(W) E0771 lung metastasis.
Statistical analysis: $*P<0,05$; $**P<0,005$; $***P<0,0005$; $****P<0,00005$. Graphs show mean ± SEM. Scale bars: 20 μm **(N, Q, T)**; 50 μm **(V)**; 100 μm **(G)**; 2,5 mm **(D)**. DAPI, 49,6-diamidino-2-phenylindole.

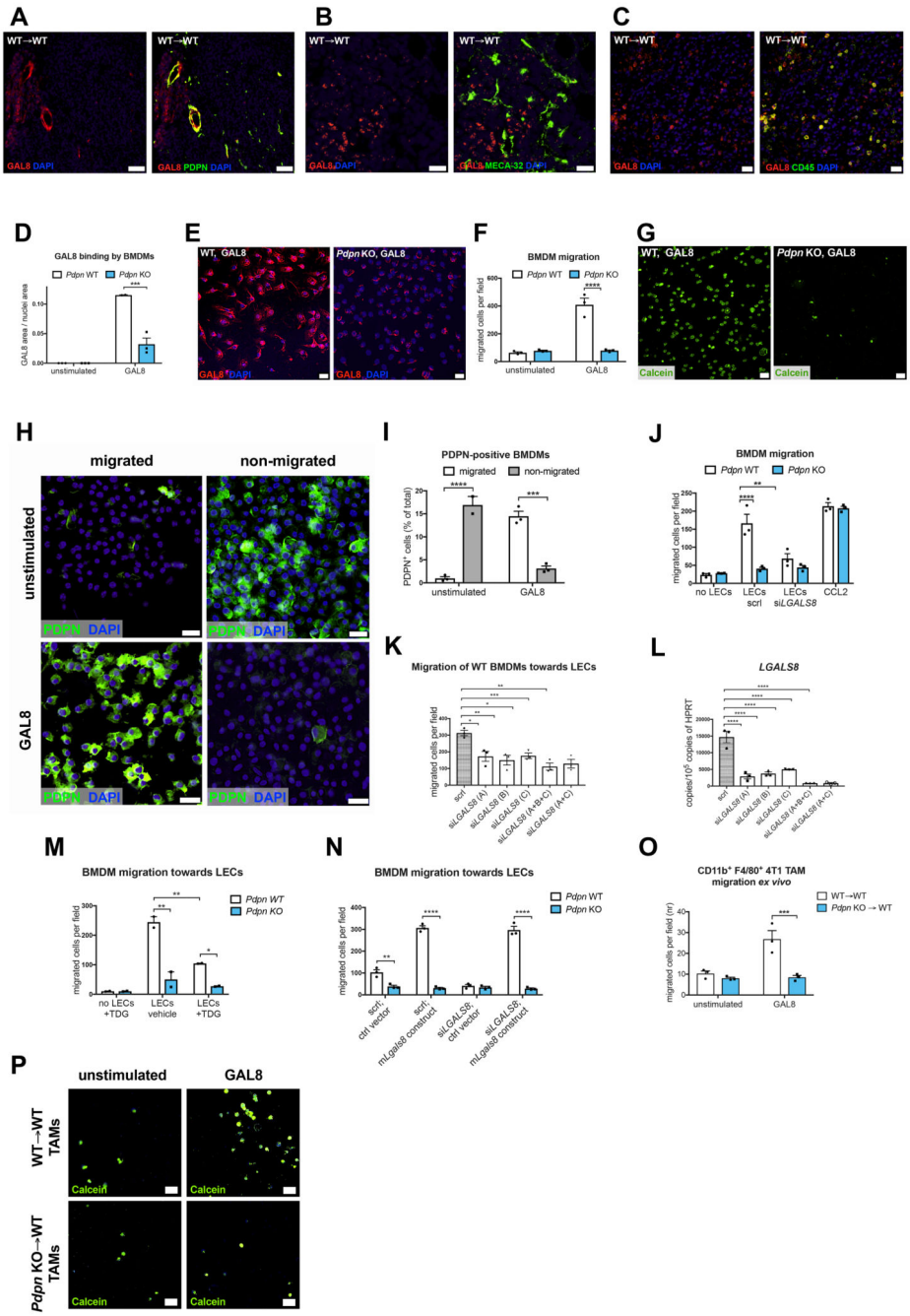

Figure 3. Perilymphatic macrophage localization is mediated by GAL8 expression in LECs.

(A-C) Representative images of 4T1 tumor sections stained for GAL8 and PDPN **(A)**, GAL8 and MECA-32 **(B)** and GAL8 and CD45 **(C)**.

(D-E) Quantification **(D)** and representative images (**E**) of WT or *Pdpn* KO BMDMs stained for GAL8 upon 40’ incubation with recombinant murine GAL8 (0,5 μM) or PBS (unstimulated).

Europe PMC Funders Author Manuscripts

(F-G) Quantification **(F)** and representative images (**G)** of WT or *Pdpn* KO Calcein-labelled BMDM migration through 8 μm pores (Transwell) in response to recombinant murine GAL8 (0,5 μM) or normal medium (unstimulated).

(H-I) Representative images **(H)** and quantification **(I)** of WT BMDM migration through 8 μm pores (Transwell) in response to murine recombinant GAL8 (0,5 μM) or normal medium (unstimulated). Migrated and non-migrated BMDM fractions were stained for PDPN and DAPI.

(J) Quantification of WT or *Pdpn* KO BMDM migration through 8 μm pores (Transwell) in response to soluble factors released by LECs (HMVECs, human microvascular endothelial cells) silenced (si*Lgals8*) or not (scrl) for *Lgals8*, a gene encoding GAL8. CCL2 was used as a positive control.

(K-L) Quantification of the migration of WT BMDMs through 8 μm pores in response to LEC-derived soluble factors **(K)**. LECs were silenced for *Lgals8* using 3 different siRNA probes separately or in combination **(L)**. scrl, scrambled control.

(M) Quantification of WT or *Pdpn* KO BMDMs migration through 8 μm pores in response to LEC-derived soluble factors. LECs were cultured with GAL8 inhibitor (TDG, 20mM). Data show representative values of two independent experiments.

(N) Quantification of WT or *Pdpn* KO BMDM migration through 8 μm pores (Transwell) in response to soluble factors released by HMVECs, silenced (si*LGALS8*) or not (scrl) for *LGALS8*, a gene encoding GAL8. Prior to the migration assay, LECs were transduced with a viral vector carrying a plasmid overexpressing murine *Lgals8* or a control plasmid (see Figure S6G-S6H).

(O-P) Quantification **(O)** and representative images **(P)** of the migration of Calcein-labelled $CD11b^+$, $F4/80^+$ TAMs sorted from 4T1 tumors bore by WT→WT and *Pdpn* KO→WT chimeras. The migration through 8 μm pores occurred in response to recombinant murine GAL8. The graph shows values of three biological repetitions per condition.

Statistical analysis: **P*<0,05; ***P*<0,005; ****P*<0,0005; *****P*<0,00005. Graphs show mean ± SEM. Scale bars: 20 μm **(B, C, E, G, H)**; 50 μm **(A, M)**. CCL2, chemokine (C-C motif) ligand 2; DAPI, 49,6-diamidino-2-phenylindole; scrl, scrambled control; LEC, lymphatic endothelial cells; TDG, thiodigalactoside.

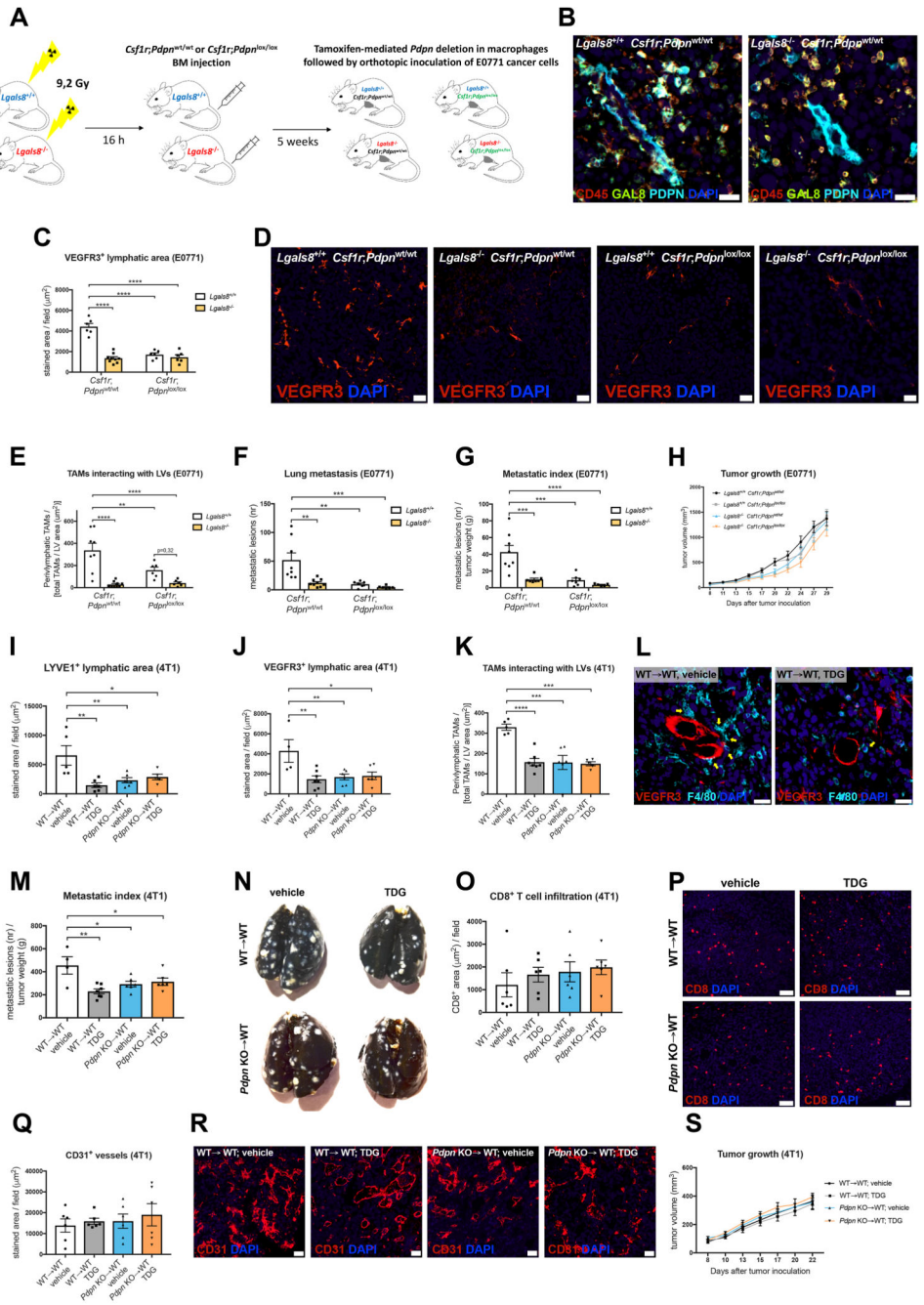

Figure 4. Genetic deletion of Lgals8 in lymphatics or pharmacologic inhibition of GAL8 prevents lymphatic growth and PoEM-dependent lymphoinvasion.

(A) Scheme illustrating generation of *Csf1r;Pdpn*$^{wt/wt}$ or *Csf1r;Pdpn*$^{lox/lox}$ chimeras upon lethal irradiation of *Lgals8*$^{+/+}$ or *Lgals8*$^{-/-}$ mice and subsequent BM reconstitution. 5 weeks after the procedure, mice were injected intraperitoneally for 5 consecutive days with 1 mg of tamoxifen in order to ensure *Pdpn* deletion in *Csf1r*$^{+}$ cells (macrophages) of the *Csf1r;Pdpn*$^{lox/lox}$ group. Next, the chimeras were orthotopically injected with E0771 breast cancer cells. Gy, Gray.

(B) Representative images of E0771 tumor sections stained for CD45, GAL8 and PDPN, demonstrating that the deletion of GAL8 in *Lgals8*$^{-/-}$ *Csf1r;Pdpn*$^{wt/wt}$ chimeras is restricted to PDPN^{+} LVs.

(C-D) Quantifications and representative images of E0771 tumor sections stained for a lymphatic endothelial cell marker VEGFR3.

(E) Quantification of F4/80^{+} TAMs directly interacting with VEGFR3^{+} LVs in E0771 tumors, assed by immunostaining.

(F-H) Lung metastasis **(F)**, metastatic index **(G)** and E0771 tumor growth **(H)** of *Csf1r;Pdpn*$^{wt/wt}$ or *Csf1r;Pdpn*$^{lox/lox}$ BM chimeras generated in *Lgals8*$^{+/+}$ or *Lgals8*$^{-/-}$ mice.

(I-J) Quantifications of 4T1 tumor sections stained for lymphatic endothelial cell markers, *i.e.* LYVE1 **(I)** and VEGFR3 **(J)**. The tumors were injected with a GAL8 inhibitor (TDG, 120 mg/kg body weight) or vehicle (PBS) 3 times per week throughout the experiment.

(K-L) Quantification **(K)** and representative images **(L)** of F4/80^{+} TAMs (yellow arrows) directly interacting with VEGFR3^{+} LVs in 4T1 tumors injected tri-weekly with TDG (120 mg/kg) or vehicle (PBS).

(M-N) Metastatic index **(M)** and representative images of black ink-injected lungs from 4T1 tumor-bearing mice **(N)**. Tumors were injected tri-weekly with TDG (120 mg/kg) or vehicle (PBS).

(O-P) Quantification **(O)** and representative images **(P)** of CD8^{+} T cells infiltrating 4T1 tumors injected tri-weekly with TDG (120 mg/kg) or vehicle (PBS).

(Q-R) Quantification **(Q)** and representative images **(R)** of CD31^{+} blood vessels in 4T1 tumors injected tri-weekly with TDG (120 mg/kg) or vehicle (PBS).

(S) 4T1 tumor growth in WT→WT and *Pdpn* KO→WT mice. The tumors were injected tri-weekly with TDG (120 mg/kg) or vehicle (PBS).

Statistical analysis: **P*<0,05; ***P*<0,005; ****P*<0,0005; *****P*<0,00005. Graphs show mean ± SEM. Scale bars: 20 μm **(B, D, L, R)**; 50 μm **(P)**.

DAPI, 49,6-diamidino-2-phenylindole; TDG, thiodigalactoside.

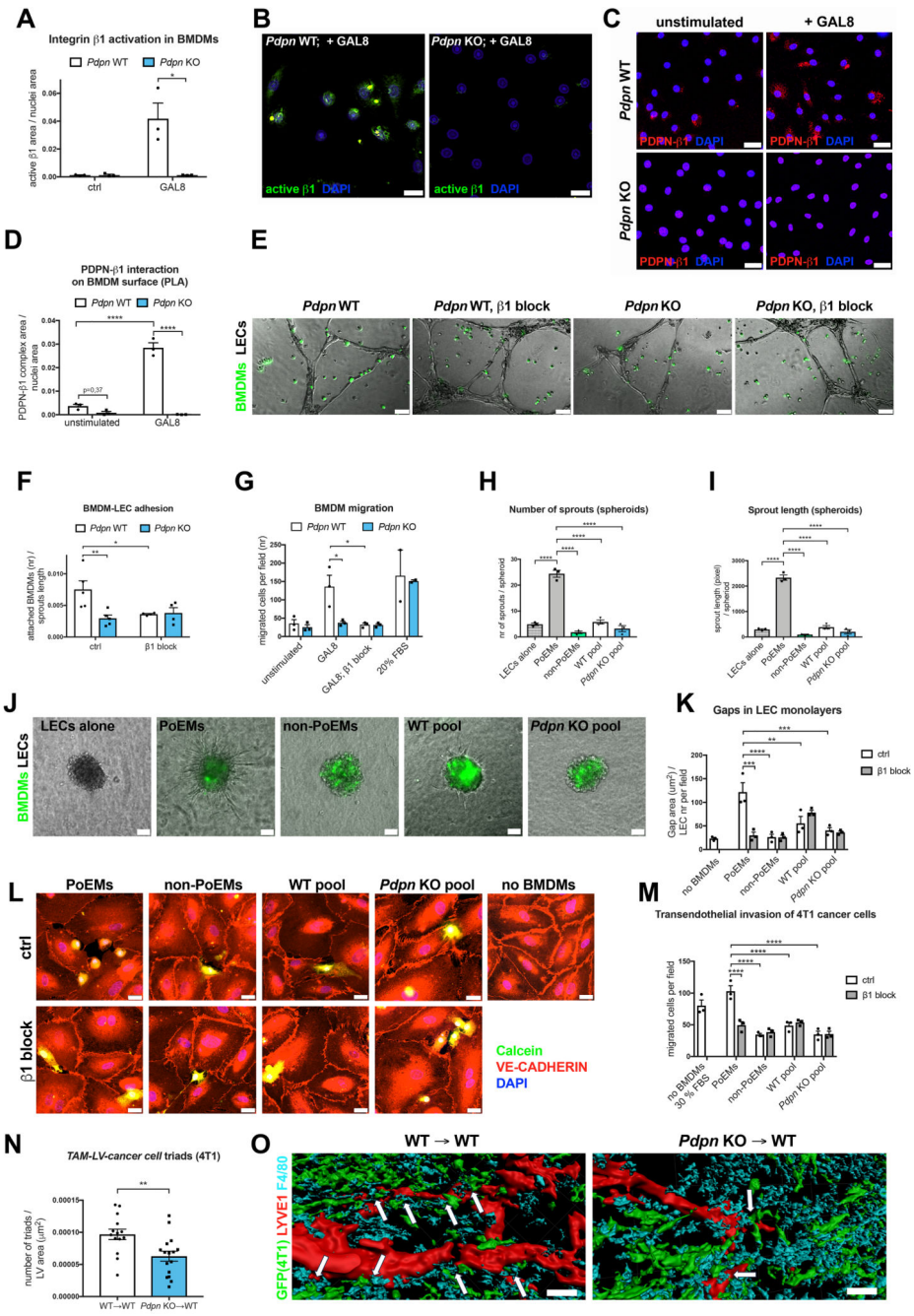

Figure 5. PDPN-mediated adhesion of PoEMs to LECs promotes lymphatic growth and cancer cell lymphoinvasion

(A-B) Quantification **(A)** and representative images **(B)** of WT or *Pdpn* KO BMDMs stained for activated form of integrin β1 (9EG7) upon 40' treatment with recombinant murine GAL8 (0,5 μM) or normal medium (ctrl).

(C-D) Representative images **(C)** and quantification **(D)** of the proximity ligation assay (PLA) between PDPN and integrin β1 on the surface of WT or *Pdpn* KO BMDMs.

Europe PMC Funders Author Manuscripts

BMDMs were treated for 40’ with recombinant murine GAL8 (0,5 μM) or normal medium (unstimulated) prior to the assay.

(E-F) Representative images **(E)** and quantification **(F)** of WT or *Pdpn* KO Calcein-labelled BMDMs adhering to preformed lymphatic capillary-like structures (HMVECs). Prior to the assay, BMDMs were incubated for 20’ with an integrin β1-blocking antibody (HMβ1-1) or with an isotype control.

(G) Quantification of *Pdpn* WT or *Pdpn* KO BMDM migration through 8 μm pores (Transwell) in response to murine recombinant GAL8 (0,5 μM). Prior to the migration, BMDMs were incubated for 20’ with an integrin β1 blocking antibody (HMβ1-1) or with an isotype control.

(H-J) Quantifications of the number of sprouts **(H)**, total sprout length **(I)** and representative images **(J)** LEC (HMVEC) spheroids embedded in collagen 1 with different sorted BMDM populations (or alone) for 24 h.

(K-L) Quantification **(K)** and representative images **(L)** of intercellular gaps between HMVECs cultured in monolayers for 5 days and incubated together with different populations of sorted, Calcein-labelled BMDMs for 16 h. The co-cultures were fixed and stained for VE-CADHERIN, enabling the visualization of cell-cell junctions.

(M) Quantification of Calcein-labelled 4T1 cancer cell migration through LEC monolayers (seeded on 8 μm pore-Transwells) incubated for 16 h with different populations of sorted BMDMs. Prior to the assay, BMDMs were incubated for 20’ with an integrin β1 blocking antibody (HMβ1-1) or with an isotype control.

(N-O) Quantification **(N)** and representative 3D reconstructions **(O)** of confocal images of 4T1-GFP^{+} tumor sections stained for LYVE1, F4/80 and GFP. White arrows demonstrate the presence of TAMs-LVs-4T1 cancer cells triads. The numbers of triads were normalized per LYVE1^{+} lymphatic vessel area. The average number of triads per tumor and total lymphatic vessel area are shown in Figure S6T-S6U.

Statistical analysis: *P<0,05; **P<0,005; ***P<0,0005; ****P<0,00005. Graphs show mean ± SEM. Scale bars: 20 μm **(B, C, E, L)**; 40 μm **(O)**.

DAPI, 49,6-diamidino-2-phenylindole; PoEMs, Podoplanin-expressing macrophages; non-PoEMs, Podoplanin-negative macrophages.

Europe PMC Funders Author Manuscripts

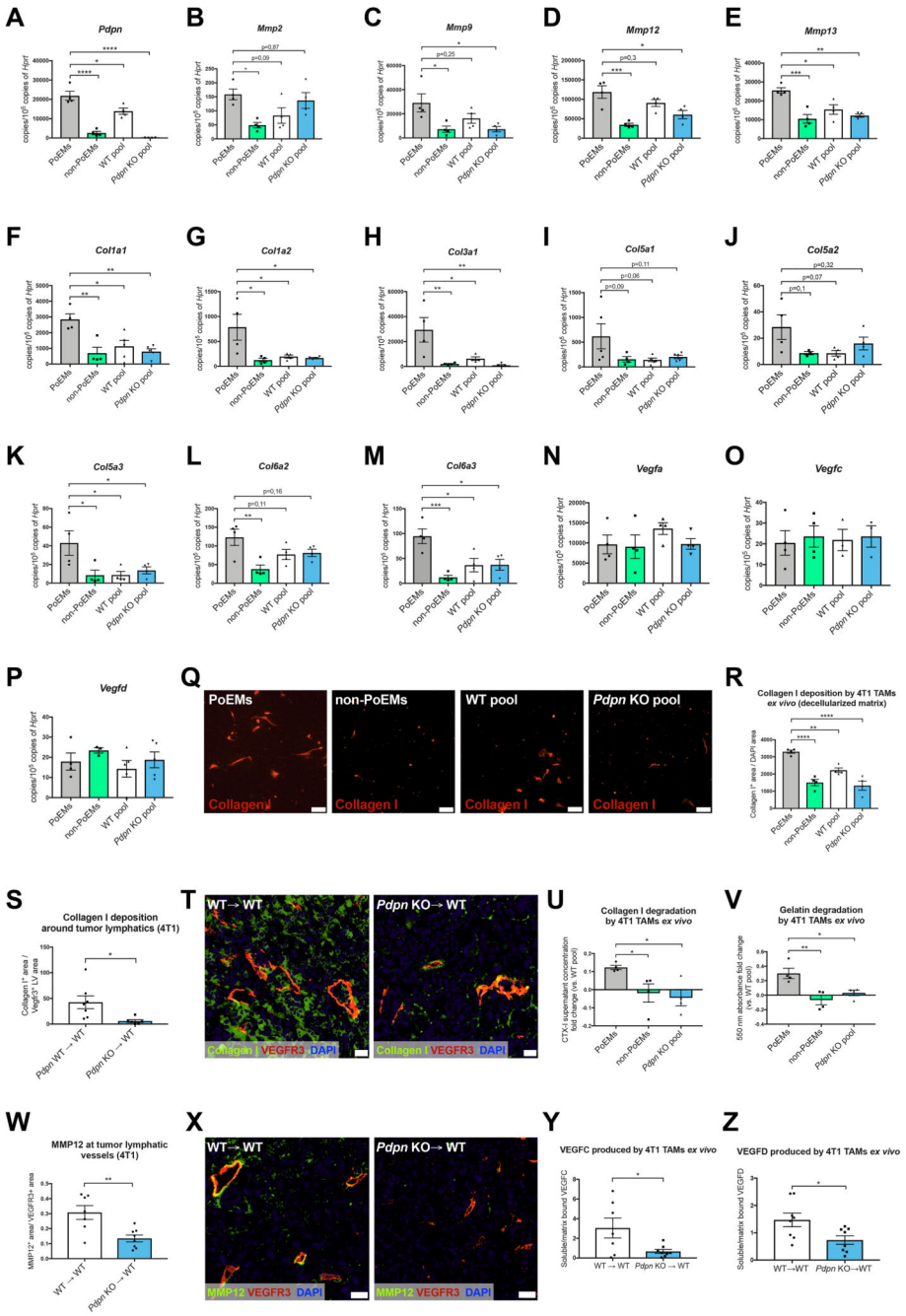

Figure 6. PDPN in PoEMs is the upstream regulator of matrix remodeling, independent of GAL8 binding

(A-M) qRT-PCR analysis of the expression of *Mmps* and *collagen* subunits in CD11b^{+}, F4/80^{+} TAM populations sorted from 4T1 tumors: PoEMs (PDPN^{+}), non-PoEMs (PDPN^{-}), total WT TAM pool and total *Pdpn* KO TAM pool (PDPN^{-}).

(N-P) qRT-PCR analysis of the expression of different *vascular endothelial growth factors* in CD11b^{+}, F4/80^{+} TAM populations sorted from 4T1 tumors: PoEMs (PDPN^{+}), non-PoEMs (PDPN^{-}), total WT TAM pool and total *Pdpn* KO TAM pool (PDPN^{-}).

(Q-R) Representative images **(Q)** and quantifications **(R)** of Collagen I deposition (on decellularized matrix) by sorted 4T1 TAMs cultured *ex vivo* for 72 h, as assessed by IF.
(S-T) Representative images **(S)** and quantifications **(T)** of Collagen I deposition around VEGFR3$^+$ lymphatics in 4T1 tumors. The collagen I$^+$ areas were normalized per VEGFR3$^+$ LV area in each field.
(U) Quantification of collagen I digestion by different 4T1 TAM populations cultured *ex vivo* for 72h, as assed by ELISA recognizing CTX-1 peptide in culture supernatants. The CTX-1 antigen concentrations were normalized *vs.* the mean concentration detected in the WT pool group. CTX-1, type I collagen cross-linked C-telopeptide.
(V) Quantification of gelatin digestion by different 4T1 TAM populations cultured *ex vivo* for 72h, as assessed spectrophotometrically with the use of direct quenched (DQ), fluorescein-labelled gelatin. The presence of green fluorescence (indicating proteolytic digestion) was assessed in culture supernatants at 485 nm.
(W-X) Representative images **(W)** and quantifications **(X)** of the MMP12$^+$ areas around VEGFR3$^+$ LVs in 4T1 tumors.
(**Y-Z**) Quantification of VEGFC **(Y)** and VEGFD **(Z)** produced by 4T1 TAMs cultured *ex vivo* for 72 h on gelatin, as assessed by ELISA. The data are shown as the ratios of VEGFC or VEGFD concentrations in supernatants (soluble) *vs.* in gelatin (matrix-bound). VEGFC, vascular endothelial growth factor C; VEGFD, vascular endothelial growth factor D. Statistical analysis: **P*<0,05; ***P*<0,005; ****P*<0,0005; *****P*<0,00005. Graphs show mean ± SEM. Scale bars: 20 μm **(Q, T, X)**.
IF, immunofluorescence; PoEMs, Podoplanin-expressing macrophages; non-PoEMs, Podoplanin-negative macrophages; DAPI, 49,6-diamidino-2-phenylindole.

Europe PMC Funders Author Manuscripts

Europe PMC Funders Author Manuscripts

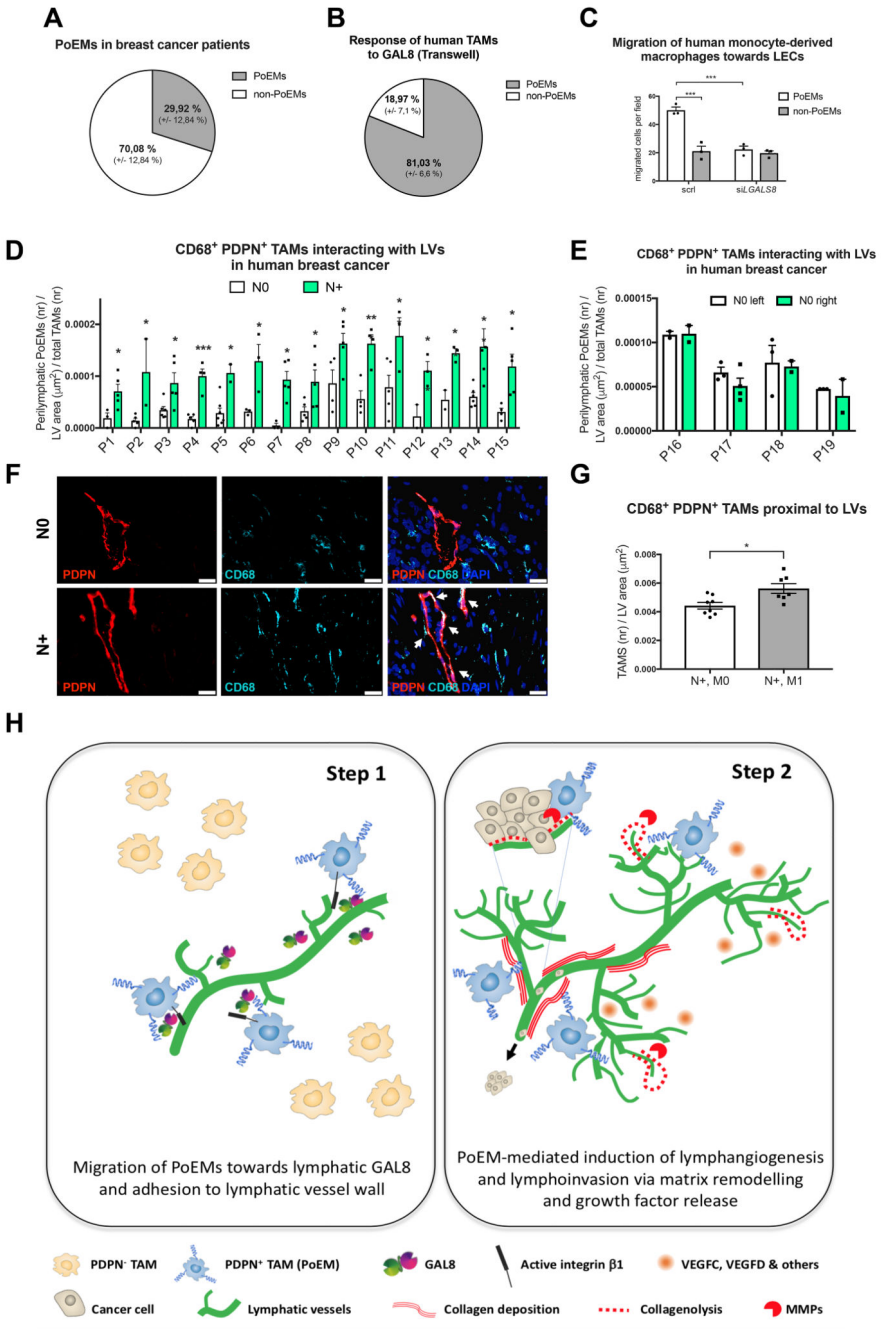

Figure 7. Potential clinical relevance of PoEMs in breast cancer patients.

(A) FACS analysis of PDPN in human breast cancer macrophages (CD11b$^+$, CD14$^+$, HLA-DR$^+$), representing the fraction of PoEMs out of total TAMs.

(B) Quantification of PDPN$^+$ cells (IF) among CD11b$^+$, CD14$^+$, HLA-DR$^+$ TAMs (sorted from human breast tumor specimens) that have migrated through 8 µm pores (Transwell) towards murine recombinant GAL8 (0,5 µM).

(C) Quantification of the migration of human monocyte-derived macrophages (CD11b$^+$, CD14$^+$) through 8 µm pores (Transwell) in response to soluble factors released by

HMVECs. LECs were silenced (si*Lgals8*) or not (scrl) for *Lgals8*, a gene encoding GAL8. scrl, scrambled control.

(D-G) IF analysis of $CD68^+$, $PDPN^+$ TAMs interacting with $PDPN^+$ LVs in paraffin-embedded human breast cancer samples obtained from patients with bilateral tumors, where N0 indicates lack and N+ presence of lymph node metastasis **(D-F)**. In N+ positive tumors, the number of $CD68^+$, $PDPN^+$ TAMs interacting with $PDPN^+$ LVs was subsequently correlated with the presence of distant organ metastasis **(G)**.

(**H**) In breast cancer, PDPN-expressing macrophages (PoEMs) represent 30% of the entire TAM population. Due to the highest expression of galectin 8 (GAL8) by the lymphatic vessels, PoEMs selectively migrate and interact with the lymphatic endothelium by means of PDPN expression. Binding of GAL8 to PDPN unleashes the clustering and activation of integrin β1, which is required for the chemotactic attraction and adhesion of PoEMs to lymphatic walls. Once there, PoEMs favor lymphangiogenesis via matrix remodeling and growth factors release. Next, they assist the intravasation of cancer cells into the lymphatic circulation, directly promoting tumor metastasis. Targeting PDPN on macrophages or GAL8 on the lymphatics efficiently impairs this cascade.

Statistical analysis: **P*<0,05; ***P*<0,005; ****P*<0,0005. Graphs show mean ± SEM. Scale bar: 20 μm **(F)**. PoEMs, Podoplanin-expressing macrophages; IF, immunofluorescence; N0, lymph node-negative; N+, lymph node-positive; P, patient; scrl, scrambled control.